Optimization of benzoxazole-based inhibitors of *Cryptosporidium parvum* inosine 5′-monophosphate dehydrogenase

Suresh Kumar Gorla[†,#], **Mandapati Kavitha**[†,#], **Minjia Zhang**[†], **James En Wai Chin**[†], **Xiaoping Liu**[‡], **Boris Striepen**[‡], **Magdalena Makowska-Grzyska**[||], **Youngchang Kim**[||], **Andrzej Joachimiak**[||], **Lizbeth Hedstrom**[†,¶], and **Gregory D. Cuny**[§,£,*]

[†]Department of Biology, Brandeis University, 415 South St., Waltham, MA 02454

[¶]Department of Chemistry, Brandeis University, 415 South St., Waltham, MA 02454

[‡]Center for Tropical and Emerging Global Diseases and Department of Cellular Biology, University of Georgia, Athens, GA 30602

[||]Center for Structural Genomics of Infectious Diseases, Computational Institute, University of Chicago, Chicago, IL 60557

[§]Laboratory for Drug Discovery in Neurodegeneration, Brigham & Women's Hospital, Harvard Medical School, 65 Landsdowne Street, Cambridge, MA 02139

[£]Department of Pharmacological and Pharmaceutical Sciences, College of Pharmacy, University of Houston, 549A Science and Research Building 2, Houston, TX 77204

Abstract

Cryptosporidium parvum is an enteric protozoan parasite that has emerged as a major cause of diarrhea, malnutrition and gastroenteritis as well as posing a potential bioterrorism threat. *C. parvum* synthesizes guanine nucleotides from host adenosine in a streamlined pathway that relies on inosine 5′-monophosphate dehydrogenase (IMPDH). We have previously identified several parasite-selective *C. parvum* IMPDH (*Cp*IMPDH) inhibitors by high-throughput screening. In this paper, we report the structure-activity relationship (SAR) for a series of benzoxazole derivatives with many compounds demonstrating *Cp*IMPDH IC_{50} values in the nanomolar range and > 500-fold selectivity over human IMPDH (hIMPDH). Unlike previously reported *Cp*IMPDH inhibitors, these compounds are competitive inhibitors versus NAD^+. The SAR study reveals that pyridine and other small heteroaromatic substituents are required at the 2-position of the benzoxazole for potent inhibitory activity. In addition, several other SAR conclusions are highlighted with regard to the benzoxazole and the amide portion of the inhibitor, including preferred stereochemistry. An x-ray crystal structure of a representative E•IMP•inhibitor complex is also presented. Overall, the secondary amine derivative **15a** (**Q67**) demonstrated excellent *Cp*IMPDH inhibitory activity (IC_{50} = 0.5 ± 0.1 nM) and moderate stability ($t_{1/2}$ = 44 min) in mouse liver microsomes. Compound **73**, the racemic version of **15a**, also displayed superb antiparasitic activity in a *Toxoplasma gondii* strain that relies on *Cp*IMPDH (EC_{50} = 20 ± 20 nM), and selectivity versus a wild-type *T. gondii* strain (200-fold). No toxicity was observed (LD_{50} > 50 μM) against a panel of four mammalian cells lines.

Corresponding author information: gdcuny@central.uh.edu, Tel no.: 1-713-743-1274.
[#]Author Contributions: These authors contributed equally.

Introduction

Cryptosporidiosis is an intestinal diarrheal disease most commonly caused by *Cryptosporidium parvum* and *hominis.* These protozoan parasites are widely distributed in both the developing and developed worlds[1] and a major cause of severe diarrhea and malnutrition in children[2]. Infection is self-limiting in immune-competent adults, but chronic in immunocompromised individuals and children. Infections are transmitted by the fecal to oral route through drinking and recreational waters[3]. The infectious oocysts are resistant to standard water treatment methods like bleach and filtration. *C. parvum* oocysts are readily obtained from infected calves, and could potentially be used as a bio-weapon [4]. Hence, *C. parvum* is categorized as a class B bio-warfare agent. Furthermore, currently available drugs are not effective for treating cryptosporidiosis and vaccine therapy is lacking[5], so new drugs are needed.

Cryptosporidium are intracellular parasites. Genomic analysis revealed that these parasites cannot synthesize purine nucleotides *de novo*, but instead salvage adenosine from the host[6]. Adenosine is converted into guanine nucleotides in a streamlined pathway that relies on inosine 5′-monophosphate dehydrogenase (IMPDH) catalyzing the conversion of inosine 5′-monophosphate (IMP) to xanthosine 5′-monophosphate (XMP) [7]. The parasite enzyme (*Cp*IMPDH) is structurally distinct from mammalian IMPDHs. *Cryptosporidium* appears to have obtained its IMPDH gene from bacteria via lateral gene transfer[6b, 6c, 8]. Therefore, *Cp*IMPDH has emerged as an attractive molecular target for the development of effective therapeutics for the treatment of diseases associated with this recalcitrant organism.

As previously reported, a high throughput screening campaign identified structurally diverse selective *Cp*IMPDH inhibitors[9]. Several of these compound series have been optimized to produce low nanomolar *Cp*IMPDH inhibitors such as **A110**, **C64**, **C97**, **P96** and **D48** (Figure 1)[10]. Herein, we report the structure-activity relationship for the benzoxazole-based inhibitor **1**, a co-crystal structure of a representative derivative of this compound series with *Cp*IMPDH and anti-parasitic activity for a subset of compounds in a *Toxoplasma gondii* surrogate model.

Results and Discussion

Chemistry

Various derivatives of **1** were synthesized using the methods depicted in Scheme 1. 5-Nitro-2-arylbenzoxazoles **3** were prepared from 2-amino-4-nitrophenols **2** and aromatic aldehydes in the presence of activated carbon (DarcoKB)[11]. Reductive hydrogenation of **3** in the presence of 10% Pd-C provided 5-amine-2-arylbenzoxazoles **4**. Substituted phenols and anilines were converted to the corresponding ethers and amines **6** upon treatment with ethyl 2-bromopropionates in the presence of K_2CO_3. Enantiomerically pure phenyl ethers were synthesized by using Mitsunobu reaction conditions with (+)-methyl D-lactate or (-)-methyl L-lactate[10a]. Ester hydrolysis was carried out in THF with 3M sodium hydroxide for racemic esters and with 3N HCl in THF for enantiomerically pure esters to yield acids **7**. Subsequently, **7** was coupled with 5-amine-2-arylbenzoxazoles **4** with the aid of EDCI•HCl in anhydrous DMF yielding amides **8**. N-alkylation of the amide was carried using sodium hydride and iodomethane to give **9** in moderate yield.

Enantiomerically pure benzoxazole amines were prepared using the method outlined in Scheme 2. L-alanine (**10**) was allowed to react with 2,3-di-chloroiodobenzene in the presence of CuI and Cs_2CO_3 to give **11** [12]. The acid was coupled with a benzoxazole amine derivative with the aid of EDCI•HCl to give **15a**. Copper (II) acetate mediated coupling of L-alanine methyl ester with 1-naphthyl boronic acid (**12**) yielded **13**[13]. Hydrolysis under

mild basic conditions generated acid **14**, which was subsequently coupled with a 5-amine-2-(4-pyridyl)benoxazole to yield **15b**.

An analogue of **1** lacking the ether oxygen was prepared following the synthetic procedure outlined in Scheme 3. 2,3-Dichlorophenylacetic acid (**16**) was treated with thionyl chloride to give the corresponding acid chloride **17**. (*R*)-4-Benzyl-2-oxazolidinone (**18**) was deprotonated with *n*-butyllithium at –78 °C, and then the generated anion was quenched with **17** to give **19**[14]. Diastereoselective methylation of **19** was carried out by treating this substrate with 1M solution of sodium bis(trimethylsilyl)amide at –78 °C, followed by the addition of iodomethane to give **20** with excellent diastereoselectivity[14]. Hydrolysis of **20** with lithium peroxide at lower temperature gave acid **21**, which was subsequently converted to amide **22**.

Replacement of the amide functional group of **1** with a bioisosteric 1,2,3-triazole was also investigated. This strategy had previously been successful with one structural class of *Cp*IMPDH inhibitors[10a], but not with another.[10d] The 1,2,3-triazole derivative of **1** was prepared according to the method depicted in Scheme 5. Propargyl ether **28** was synthesized using a Mitsunobu procedure. Then 2-(thiazol-5-yl)benzo[d]oxazol-5-amine (**4**, R_1 = 5-thiazole, X = H) was converted to the corresponding diazonium chloride followed by quenching with sodium azide to yield **29**. Finally, a CuI mediated reaction of alkyne **28** with azide **29** gave **30** [15].

An analogue in which the benzoxazole ring was replaced with a 1,3-diamide was generated using the method outlined in Scheme 6. 3-Nitroaniline **31** was coupled with isonicotinic acid to yield amide **32**. Tin mediated reduction of **32** gave **33**, which was coupled with (*S*)-2-(3,4-di-chlorophenoxy) propionic acid to generate **34**.

Regioisomers of **1** were prepared using the procedures outlined in Scheme 8. 2-Amino-5-nitrophenol (**37**) and aromatic aldehydes were condensed and oxidized in the presence of activated carbon (DarcoKB) to give **38**[11]. Reductive hydrogenation of **38** in presence of 10% Pd-C provided 6-amino-2-aryl benzoxazoles **39**. Subsequently, amines **39** were coupled with (*S*)-2-(2,3-di-chlorophenoxy) propionic acid with the aid of EDCI•HCl to yield **40.**

Evaluation of *Cp*IMPDH inhibition

*Cp*IMPDH and hIMPDH2 were expressed and purified as previously described (note that *C. hominis* IMPDH is identical to *Cp*IMPDH)[16]. Enzymatic activity was assayed by monitoring the production of NADH[9]. IC_{50} values reported herein were determined from the average of three independent experiments, unless otherwise noted. IC_{50} values were also measured in the presence of 0.05% fatty acid free bovine serum albumin (BSA) in order to assess nonspecific protein binding[17]. Our previous experience indicates that IC_{50} values in the presence of BSA are a better predictor of antiparasitic activity[18]. None of the compounds significantly inhibited hIMPDH2 (IC_{50} >5μM).

Initially the aryl ether substituent was evaluated (Table 1). Removal of the 4-chloro group (**41**) resulted in a two-fold increase in inhibitory activity, whereas removal of the 2-chloro group (**42**) gave a two-fold loss in activity. Removal of both chlorine atoms resulted in activity comparable to the parent compound **1**. The electron donating substitution 4-OMe (**44**) demonstrated comparable activity to **41**. Translocation of the chlorine atom in **41** from the 2-position to the 3-position (**45**) was well tolerated. Combining these changes by utilizing a 2,3-di-chloro substituted phenyl ether (**46**) gave a five-fold increase in activity compared to **41** and **45**. However, the 2,6-di-chloro phenyl ether derivative **47** was devoid of activity. Transforming the 2,3-dichlorophenyl into a 1-naphthyl resulted in a potent inhibitor

(**48**) with an IC_{50} value of 9 nM, which only increased slightly in the presence of BSA. These results suggest that the sterics of this group are an important determinant for binding. However, addition of a chlorine atom to the naphthyl group in the 4-position (**49**) was detrimental.

Next, the importance of amide methylene group was examined (Table 2). Removal of the α-methyl (**50**) or addition of another α-methyl (**51**) at this position resulted in complete loss of activity. Replacing the methyl with a larger isopropyl (**52**) resulted in approximately a three-fold loss of activity compared to **48**. The enantiomers of **48** were also investigated and found to demonstrate a stereochemical preference. The (*S*)-isomer (**54**, $IC_{50} = 6.1$ nM, $IC_{50} = 8$ nM in the presence of BSA) was significantly more potent than the (*R*)-isomer (**53**, $IC_{50} = 400$ nM). Again the (*S*)-isomers of several other derivatives containing electron withdrawing groups at the 2,3-positions of the phenyl ether (**55**, **56** and **57**) demonstrated excellent *Cp*IMPDH inhibitory activities ($IC_{50} < 10$ nM). However, the (*S*)-isomer of the 2,3-di-methoxy derivative **58** was less active ($IC_{50} = 50$ nM).

The importance of the pyridine substituent was subsequently examined (Table 3). Replacing the pyridine with phenyl (**59**) resulted in complete loss of activity ($IC_{50} > 5$ YM). Translocation of the nitrogen to the 2-or 3-positions (**60** and **61**) resulted in a 3- to 4-fold loss in potency. However, evaluation of derivatives **62** and **63** indicated that a 5-thiazole was an excellent replacement of the 4-pyridyl, while the 2-thiazole (**65**) and 2-pyrrole (**66**) derivatives resulted in loss of activity compared to **55** and **54**, respectively. Finally, the 2-pyrimidine derivative **67** proved to be inactive.

Following initial assessments of the phenyl ether, the amide α-methylene and the pyridine moieties in inhibitor **1**, a variety of other changes were explored for the amide and central heterocycle (Table 4). For example, bioisosteric replacement of the amide with a 1,2,3-triazole (**30**), N-methylation of the amide nitrogen (**9**) or inversion of the amide (**36**) all resulted in loss of inhibitory activity. However, regioisomers produced by transposing the amide from the 5-position of the benzoxazole to the 6-position (**40a** and **40b**), surprisingly, resulted in compounds with excellent *Cp*IMPDH inhibitory activity ($IC_{50} < 10$ nM), although the relative effect of BSA appeared to be slightly greater compared to **55** and **62**, respectively. Addition of a chlorine atom to the 7-position of the benzoxazole of **55** resulted in **68** and significantly eroded *Cp*IMPDH inhibitory activity. Finally, replacing the benzoxazole with a benzimidazole (**26**) or opening of the oxazole ring (**34**) lead to loss of inhibitory activity.

The next perturbation examined was to replace the ether C-O bond with a C-C bond (Table 5). In the first iteration, a methylene substituted for the oxygen atom (**69**), which resulted in loss of inhibitory activity. However, deletion of the oxygen atom, generating a phenyl acetamide derivative, resulted in moderately potent inhibition (**70**, $IC_{50} = 120$ nM). Interestingly, the stereochemical preference of the phenyl acetamide derivatives was the opposite of the ether derivatives. For example, the (*S*)-isomer **71** was inactive, while the (*R*)-isomer **72** displayed an IC_{50} value of 22 nM. Another example was investigated to confirm this observation. The (*R*)-2,3-di-chlorophenyl derivative **22** was found to be a moderately potent *Cp*IMPDH inhibitor, although it was less active than the (*S*)-ether **55**.

Given the interesting results obtained with replacing the C-O bond of **1** with a C-C bond, the ether was exchanged with a secondary amine (Table 6). The 2,3-dichlorophenyl amine derivative **73** demonstrated slightly improved activity compared to the corresponding 2,3-dichlorophenyl ether **46**. In addition, the (*S*)-isomer **15a** proved to be a very potent *Cp*IMPDH inhibitor ($IC_{50} = 0.5$ nM), although the (*S*)-naphthyl amine derivative **15b** was less active ($IC_{50} = 14$ nM).

Evaluation of kinetic mechanism for *Cp*IMPDH inhibition

The high throughput screen was designed to target the cofactor site since this site is the most diverged, and therefore most likely to yield inhibitors selective for the parasite enzyme.[9] *Cp*IMPDH, like other IMPDHs characterized to date, has a kinetic mechanism wherein substrates bind randomly and hydride transfer occurs forming a covalent E-XMP* intermediate and NADH.[7] Products dissociate in an ordered fashion, with NADH release occurring before the hydrolysis and release of E-XMP*. In principle, IMPDH inhibitors that bind in the cofactor site can be competitive, uncompetitive or noncompetitive, depending on their relative affinities for the E, E•IMP and E-XMP* complexes. In practice, most such inhibitors are noncompetitive, suggesting comparable affinities for E•IMP and E-XMP*. Uncompetitive inhibition is also commonly observed, indicating a strong preference for E-XMP*. The inhibition mechanisms of four representative inhibitors (**1**, **63**, **68** and **72**) were evaluated. Surprisingly, the inhibition data with respect to NAD^+ for all four compounds were best fit by competitive mechanism (Figure 3 and Table 7). However, the fit to a noncompetitve/mixed inhibition was not significantly inferior. This ambiguity is a consequence of NAD^+ substrate inhibition, which prevents the use of saturating NAD^+ concentrations.[7] This observation suggests that these compounds have a strong preference for E•IMP. All four compounds are noncompetitive inhibitors with respect to IMP.

Mouse liver microsomal stability

A selected set of the *Cp*IMPDH inhibitors was evaluated for metabolic stability in mouse liver microsomes (Table 8). Compounds were incubated with microsomes at 37 °C in the presence and absence of NADPH. The percentage of compound remaining at various time points was determined and then the data were fit to a first-order decay model to determine half-life. Three ether derivatives (**55**, **62** and **40a**) demonstrated poor stability in both the presence and absence of NADPH ($t_{1/2}$ 12 min), whereas **54** was moderately more stable ($t_{1/2}$ = 30 min). In the case of two phenyl acetamide derivatives, the unsubstituted inhibitor **72** proved more stable ($t_{1/2}$ = 43 min) compared to the 2,3-di-chlorophenyl inhibitor **22** ($t_{1/2}$ = 25 min) in the presence of NADPH. Both compounds were quite stable in the absence of NADPH. For the amine derivatives, the 2,3-di-chlorophenyl inhibitor **15a** also displayed moderate stability in the presence of NADPH ($t_{1/2}$ = 44 min), whereas the naphthyl derivative **15b** was less stable in the presence or absence of NADPH ($t_{1/2}$ = 18 min and 27 min, respectively).

The structure of *Cp*IMPDH in complex with 54 and IMP

The structure of *Cp*IMPDH in complex with IMP and **54** was solved at 2.10 Å resolution using molecular replacement with the structure of apo *Cp*IMPDH (PDB ID code 3FFS) as the search model (Table S1). The structure (Figure 3A) revealed that the inhibitor binds in the active site and interacts with residues from two adjacent subunits, similarly as previously observed in the structure of *Cp*IMPDH with **C64** (PDB ID code 3KHJ)[10b]. This binding mode is significantly different compared to hIMPDH inhibitors and it likely accounts for the selectivity of the benzoxazole compounds. Inhibitors of mammalian IMPDH such as mycophenolic acid (MPA) bind in the nicotinamide subsite and interact directly with the purine ring of the substrate, IMP. In addition, the MPA interaction extends into the adenine subside. However, the interactions for MPA are limited to the residues within the same monomer (Figure 3B). In contrast, the naphthalene of **54** stacks against the purine ring of IMP, in a manner similar to the 2-thiazole of **C64**, with the remainder of **54** extending across the subunit interface into the pocket in the adjacent monomer. Unlike **C64**, the 2-(4-pyridyl)benzoxazole of **54** fills much of this cavity and the pyridine nitrogen of **54** participates in a water-mediated hydrogen bond with the L170 main chain amide nitrogen (Figures 3A and 4). This hydrogen bond can account for the requirement of the 4-pyridyl or

5-thiazolyl substituents. These additional interactions are likely to explain the increased affinity of **54** relative to **C64** (IC$_{50}$ = 28 nM and 6 nM for **C64** and **54**, respectively). The structure also reveals that the (*S*)-methyl group of **54** forms a hydrophobic interaction with M308. Inverting this center to the (*R*)-isomer would likely introduce a steric clash with E329, which forms a hydrogen bond with the amide NH of **54** and along with S354′ (where ′ denotes a residue from the adjacent subunit) and T221 forms a hydrogen bonding network with Y358′ (Figures 3A and 4). These observations provide a rationale for the observed stereochemical preference with regard to the substituent on the amide α-position in the ether and amine derivatives. In addition, the benzo-portion of the benzoxazole ring of **54** appears to interact with the side-chain of Y358′.

Evaluation of antiparasitic activity

Although the generation of potent *Cp*IMPDH inhibitors has been accomplished with several structurally distinct compound classes, achieving antiparasitic activity in *C. parvum* remains a challenge. This organism cannot be continuously cultured in vitro, so such assays are poor mimics of in vivo infection in addition to having a poor dynamic range. However, the related intracellular parasite *T. gondii* has proven to be a well behaved organism that can be engineered to express fluorescent markers, facilitating its use in screening.[20] Previously, we genetically engineered a *T. gondii* strain that relies on *Cp*IMPDH (Toxo/*Cp*IMPDH) to synthesize guanine nucleotides.[18] In contrast, the wild type *T. gondii* strain RH (Toxo/WT) contains a eukaryotic IMPDH that is resistant to *Cp*IMPDH inhibitors, thus providing target validation as well as a measure of host cell cytotoxicity[18].

A set of twenty-two *Cp*IMPDH inhibitors were evaluated for activity in both Toxo/ *Cp*IMPDH and Toxo/WT assays (Table 9). Four compounds (**46**, **48**, **40a** and **73**) demonstrated EC$_{50}$ values 250 nM in the Toxo/*Cp*IMPDH assay and selectivity > 30-fold versus Toxo/WT. Thus, the 2,3-dichlorophenyl or 1-naphthyl ethers or amines at either the 5- or -6-positions of the 2-(4-pyridyl)- or 2-(thiazolyl)benzoxazoles translated into encouraging antiparasitic activity. Furthermore, two of these compounds (**40a** and **73**) demonstrated EC$_{50}$ values 30 nM and selectivity > 150-fold, indicating that the 2,3-dichlorophenyl ether or amine at either the 5- or 6-positions of the 2-(4-pyridyl)benzoxazole might be preferable. Based on the in vitro and cellular properties, these compounds are candidates for evaluation in an animal model of cryptosporidiosis.

Evaluation of mammalian cytotoxicity activity

A subset of compounds (**15a**, **40a**, **41**, **44**, **46** and **57**) were also evaluated for cytotoxicity against four mammalian cell lines (HeLa, HEK293, COS and CHO). Viability was determined by monitoring metabolic activity with alamarBlue® assay. None of the compounds displayed significant toxicity (LD$_{50}$ > 50 μM) against all four cell lines, except **41** which exhibited an LD$_{50}$ ~ 12.5 μM in HEK293 cells.

Conclusions

A SAR study of *Cp*IMPDH inhibitor **1** revealed that 2,3-di-substituted phenyl ethers improved potency, while a 4-pyridyl or 5-thiazolyl group was necessary at the 2-position of the benzoxazole. In addition, the (*S*)-isomers were significantly more potent compared to the corresponding (*R*)-isomers, but the connectivity of the amide could be transposed from the 5-position of the benzoxazole to the 6-position. The ether oxygen atom could be deleted generating α-arylamides where the chiral preference switched with the (*R*)-isomer being more potent. Furthermore, the ether oxygen atom could be replaced with an NH without jeopardizing potent *Cp*IMPDH inhibitory activity and again the (*S*)-isomer was preferred. The secondary amine derivative **15a** (**Q67**) or its racemic version **73** demonstrated excellent

*Cp*IMPDH inhibitory activity in the presence or absence of BSA and moderate stability in the presence of mouse liver microsomes, as well as superb activity and selectivity in a *T. gondii* surrogate cell assay of *C. parvum* infection and no significant cytotoxicity against a panel of four mammalian cells. Finally, a co-crystal structure of *Cp*IMPDH with IMP and **54** (**Q21**) allowed for a more complete understanding of the structure-activity relationships observed with the benzoxazole inhibitors and also demonstrated that this compound series adopts a similar binding mode as a structurally distinct and previously reported *Cp*IMPDH inhibitor **C64**.[10b] This information should assist in the continuing development of *Cp*IMPDH inhibitors that will allow for further understanding of this apicomplexan parasite and its host interactions, advancing the treatment of cryptosporidiosis.

Experimental Section

Chemistry Material and Methods

Unless otherwise noted, all reagents and solvents were purchased from commercial sources and used without further purification. Compounds **1**, **50**, **51**, **60** and **61** were purchased from Chembridge Corporation (San Diego, CA 92121, USA). All reactions were performed under a nitrogen atmosphere in dried glassware unless otherwise noted. All NMR spectra were obtained using a 400 MHz spectrometer and conducted in CDCl$_3$, unless otherwise indicated. For ^{1}H NMR, all chemical shifts are reported in δ units ppm and are referenced to tetramethylsilane (TMS). All chemical shift values are also reported with multiplicity, coupling constants and proton count. Likewise, for ^{13}C NMR, all chemical shifts are reported in δ units ppm and are referenced to the central line of the triplet at 77.23 ppm for those conducted in CDCl$_3$. Coupling constants (*J* values) are reported in hertz. Column chromatography was carried out on SILICYCLE SiliaFlash silica gel F60 (40–63 μm, mesh 230–400). High-resolution mass spectra (HRMS) were obtained using a Q-tof UE521 mass spectrometer (University of Illinois, SCS, and Mass Spectrometry Lab).

HPLC conditions

All final compounds have a chemical purity >98% as determined by analysis using a Agilent 1100 HPLC instrument equipped with a quaternary pump and a Zorbax® SB-C8 column (30 × 4.6 mm, 3.5 mm). UV absorption was monitored at 254 nm. The injection volume was 5 μL. HPLC gradient was 5 % acetonitrile and 95 % water (both solvents contain 0.1% trifluoroacetic acid) with a total run time of 2.5 min and a flow rate of 3.0 mL/min.

Enantiomeric purity was determined using HPLC analysis on a Agilent 1100 Series instrument equipped with a quaternary pump using a Chiralpak AS-H Column (250 × 4.6 mm) for all chiral compounds unless noted. The UV absorption was monitored at 254 nm and the injection volume was 10 μL. A Chiralpak OD-H column was used for **22**, **40a**, **40b** and **58**, and an OJ-H column was used for **15b**, **73** and **74**. For these latter two columns the UV absorption was monitored at 220 nm and an injection volume 20 μL was used. HPLC gradient for all compounds was 70 % n-hexane and 30 % *i*-propanol and a flow rate of 1.0 mL/min.

General procedure for the preparation of 5-nitro-2-arylbenzo[d]oxazoles (3). Exemplified for 5-nitro-2-(pyridine-4-yl)benzo[d]oxazole (3, R$_1$ = 4-Py, X = H)— To a solution of 2-amino-4-nitrophenol (500 mg, 3.24 mmol) in anhydrous xylene (10 mL) in a 100 mL three-neck flask under an oxygen atmosphere was added 4-pyridine carboxaldehyde (347 mg, 3.23 mmol) and Darco KB (600 mg). The solution was stirred at 120 °C for 4 h. The reaction mixture was allowed to cool to room temperature and then filtered with the aid of Celite. The filtrate was concentrated and the residue was purified by silica gel column chromatography using a mixture of ethyl acetate/*n*-hexane (50:50) to give

5-nitro-2-(pyridine-4-yl)benzo[d]oxazole (600 mg, 77%) as a yellow solid. ^{1}H NMR (CDCl$_3$, 400 MHz) δ 7.76 (d, J = 9.2 Hz, 1H), 8.11 (d, J = 6 Hz, 2H), 8.40 (d, J_1 = 12 Hz, J_2 = 2.4 Hz, 1H), 8.73 (d, J = 2 Hz, 1H), 8.89 (d, J = 6 Hz, 2H).

General procedure for the preparation of 5-amino-2-aryl-benzo[d]oxazoles (4). Exemplified for 5-amino-2-(pyridine-4-yl)benzo[d]oxazole (4, R$_1$ = 4-Py, X = H) —To a solution of 5-nitro-2-(pyridine-4-yl)benzo[d]oxazole (600 mg, 2.48 mmol) in ethyl acetate/MeOH (1:1, 10 mL) was added a catalytic amount of 10% Pd-C. The reaction mixture was placed under a hydrogen atmosphere and stirred for 6 h at room temperature. The mixture was then filtered, concentrated and the residue purified by flash column chromatography on silica gel using 100% ethyl acetate as eluent to afford 5-amino-2-(pyridine-4-yl)benzo[d]oxazole (450 mg, 86%) as a yellow solid. ^{1}H NMR (CDCl$_3$, 400 MHz) δ 6.78 (dd, J_1 = 12 Hz, J_2 = 2.4 Hz, 1H), 7.07 (d, J = 2 Hz, 1H), 7.40 (d, J = 4.8 Hz, 1H), 8.05 (dd, J_1 = 8 Hz, J_2 = 1.6 Hz, 2H), 8.79 (dd, J_1 = 4 Hz, J_2 = 1.6 Hz, 2H), 3.78 (s, 2H).

General procedure for the preparation of (±)-7. Exemplified for 2-(2,3-dichlorophenoxy)propionic acid (7, R$_2$ = 2,3-di-ClPh, R$_3$ = Me, Y = O)—To a solution of 2,3-dichlorophenol (200 mg, 1.22mmol) in anhydrous DMF (15 mL) was added K$_2$CO$_3$ (505 mg, 3.66 mmol) and ethyl 2-bromopropionate (287.1 mg, 1.58 mmol). The reaction mixture was stirred at room temperature for 5 h under a nitrogen atmosphere, diluted with water (50 mL) and extracted with ethyl acetate (3 X 50 mL). Note, when Y = NH this reaction was conducted at 70 °C for 3 h. The organic extracts were combined, washed with brine, dried over anhydrous MgSO$_4$, filtered and concentrated in vacuo. The residue was purified by silica gel column chromatography using a mixture of ethyl acetate and *n*-hexane (10:90) to give ethyl 2-(2,3-dichlorophenoxy)propionate (290 mg, 1.2 mmol, 90%) as a colorless liquid. The ester (290 mg, 1.60 mmol) was dissolved in THF: H$_2$O (2:1), and then NaOH (132 mg, 3.3 mmol) was added. The reaction mixture was heated at 80 °C for 3 h. After the reaction mixture was allowed to cool to room temperature, 1N HCl was added until a pH of 7 was reached and then the mixture was extracted with DCM. The organic layers were dried over anhydrous MgSO$_4$, filtered, and concentrated. The residue was purified by silica gel column chromatography using a mixture of ethyl acetate/*n*-hexane (60:40) to afford 2-(2,3-dichlorophenoxy)propionic acid (270 mg, 95%) as a white solid.

General procedure for the preparation of (*R*)- and (*S*)-7. Exemplified for (*S*)-2-(2,3-dichlorophenoxy)propionic acid (7, R$_2$ = 2,3-di-ClPh, R$_3$ = (*S*)-Me, Y = O)— 2,3-Dichlorophenol (150 mg, 0.92 mmol) was dissolved in anhydrous DCM (6 mL) under a nitrogen atmosphere and then methyl (*R*)-(+)-2-(4-hydroxyphenyl)propionate (143.7 mg, 1.38 mmol) was added. After the reaction mixture was cooled to 0 °C, PPh$_3$ (289.4 mg, 1.10 mmol) was added portion-wise and the reaction mixture was stirred for 10 minutes. Then DEAD (240 mg, 1.37 mmol) was slowly added. The reaction mixture was stirred for 12 h at room temperature and then 10 mL of water was added and the mixture extracted with DCM. The organic layers were washed with brine, dried over anhydrous MgSO$_4$, filtered and concentrated. The residue was purified by column chromatography on silica gel using ethyl acetate/*n*-hexane (10:90) to yield methyl (*S*)-2-(2,3-dichlorophenoxy)propionate (180 mg, 0.76 mmol, 83%) as a colorless liquid. The ester (180 mg, 0.72 mmol) was added to a mixture of 6 mL THF in 3N HCl (2:8), and then heated at 70 °C for 6 h. The reaction mixture was allowed to cool to room temperature then extracted with DCM. Organic layers were washed with brine, dried over anhydrous MgSO$_4$, filtered, and concentrated. The residue was purified by silica gel column chromatography using ethyl acetate/*n*-hexane (60:40) to afford (*S*)-2-(2,3-dichlorophenoxy)propionic acid (110 mg, 62%) as a white

solid. ^{1}H NMR (CDCl$_3$, 400 MHz) δ 1.51(d, J = 7.2 Hz, 3H), 4.27 (q, J = 7.2 Hz, 1H), 7.16 – 7.24 (m, 2H), 7.37 (dd, J_1 = 3.6 Hz, J_2 = 1.6 Hz, 1H).

General procedure for the preparation of benzoxazoles (8). Exemplified for (*S*)-2-(2,3-dichlorophenoxy)-*N*-(2-(pyridin-4-yl)benzo[d]oxazol-5-yl)propionamide (55)—To a solution of 5-amino-2-(pyridine-4-yl)benzo[d]oxazole (266.7 mg, 1.27 mmol) and (*S*)-2-(2,3-dichlorophenoxy)propionic acid (300 mg, 1.27 mmol) were dissolved in anhydrous DMF (5 mL) under a nitrogen atmosphere. The reaction mixture was cooled to 0 °C and then EDCI•HCl (489.6 mg, 2.55 mmol) was added. The reaction mixture was stirred for 12 h at room temperature. Volatiles were removed under reduced pressure and the mixture was dissolved in 20 mL DCM. The organic layer was washed sequentially with a saturated aqueous solution of sodium bicarbonate and brine. The organic layers were dried over anhydrous MgSO$_4$, filtered, and concentrated. The residue was purified by silica gel column chromatography using ethyl acetate/*n*-hexane (50:50) to give **55** (390 mg, 72%) as a white solid. ^{1}H NMR (CDCl$_3$, 400 MHz) δ 1.76 (d, J = 6.8 Hz, 3H), 4.90 (q, J = 6.8 Hz, 1H), 6.93 (dd, J_1 = 7.2 Hz, J_2 = 2.4 Hz, 1H), 7.17 – 7.23 (m, 2H), 7.56 – 7.61 (m, 2H), 8.06 (dd, J_1 = 4 Hz, J_2 = 1.6 Hz, 2H), 8.17 (s, 1H), 8.81 – 8.83 (m, 3H); ^{13}C NMR (CDCl$_3$, 100 MHz) δ 18.6, 76.9, 111.2, 112.1, 113.2, 119.2, 121.2, 122.9, 124.3, 128.1, 134.3, 134.5, 134.7, 142.4, 148.0, 150.9, 153.7, 161.8, 169.2; ESIHRMS for C$_{21}$H$_{16}$N$_3$O$_3$Cl$_2$ (M+H)$^{+}$ calcd. 428.0569, found 428.0568, Chiral purity (% ee > 98, t_R=12.84 min).

The following compounds were prepared in a similar manner:

2-(2-chlorophenoxy)-*N*-(2-(pyridine-4-yl)benzo[d]oxazol-5-yl)propionamide (41): 71%; white solid; ^{1}H NMR (CDCl$_3$, 400 MHz) δ 1.77 (d, J = 6.4 Hz, 3H), 4.90 (q, J = 6.8 Hz, 1H), 7.02 (t, J = 7.6 Hz, 2H), 7.25 – 7.29 (m, 1H), 7.45 (d, J = 8 Hz, 1H), 7.57 (d, J = 8.4 Hz, 1H), 7.64 (dd, J_1 = 8 Hz, J_2 = 2 Hz, 1H), 8.06 (d, J = 5.2 Hz, 2H), 8.17 (s, 1H), 8.82 (d, J = 4.4 Hz, 2H), 8.95 (s, 1H); ^{13}C NMR (CDCl$_3$, 100 MHz) δ 18.7, 76.8, 111.1, 111.9, 115.6, 119.2, 121.1, 123.5, 123.8, 128.4, 130.8, 134.3, 134.9, 142.3, 147.9, 150.9, 152.4, 161.7, 169.5; ESI-HRMS for C$_{21}$H$_{17}$N$_3$O$_3$Cl (M+H)$^{+}$ calcd. 394.0958 found 394.0961.

2-(4-chlorophenoxy)-*N*-(2-(pyridine-4-yl)benzo[d]oxazol-5-yl)propionamide (42): 72%; white solid; ^{1}H NMR (CDCl$_3$, 400 MHz) δ 1.69 (d, J = 6.8 Hz, 3H), 4.79 (q, J = 6.8 Hz, 1H), 6.94 (d, J = 8.8 Hz, 2H), 7.30 (d, J = 8.4 Hz, 2H), 7.51 – 7.58 (m, 2H), 8.08 (dd, J_1 = 10 Hz, J_2 = 2 Hz, 3H), 8.29 (s, 1H), 8.82 (d = 4.8 Hz, 2H); ^{13}C NMR (CDCl$_3$, 100 MHz) δ 18.8, 76.0, 111.2, 112.5, 117.3, 119.5, 121.2, 127.8, 130.1, 134.3, 134.5, 142.4, 148.1, 150.9, 155.3, 161.8, 170.1; ESI-HRMS for C$_{21}$H$_{17}$N$_3$O$_3$Cl (M+H)$^{+}$ calcd. 394.0958 found 394.0961.

2-phenoxy-*N*-(2-(pyridine-4-yl)benzo[d]oxazol-5-yl)propionamide (43): 63%; white solid; ^{1}H NMR (CDCl$_3$, 400 MHz) δ 1.69 (d, J = 6.4 Hz, 3H), 4.84 (q, J = 6.4 Hz, 1H), 7.07 – 6.99 (m, 3H), 7.34 (t, J = 8 Hz, 2H), 7.54 (t, J = 8.4 Hz, 2H), 8.08 (d, J = 13.6 Hz, 3H), 8.42 (s, 1H), 8.82 (s, 2H); ^{13}C NMR (CDCl$_3$, 100 MHz) δ 18.9, 75.6, 111.1, 112.4, 115.9, 119.6, 120.5, 121.2, 121.2, 121.3, 122.7, 128.1, 130.1, 134.3, 134.6, 142.4, 148.0, 150.9, 156.8, 161.7, 170.6; ESI-HRMS for C$_{21}$H$_{18}$N$_3$O$_3$ (M+H)$^{+}$ calcd. 360.1348, found 360.1350.

2-(4-methoxyphenoxy)-*N*-(2-(pyridine-4-yl)benzo[d]oxazol-5-yl)propionamide (44): 73%; white solid; ^{1}H NMR (CDCl$_3$, 400 MHz) δ 1.66 (d, J = 6.8 Hz, 3H), 3.78 (s, 3H), 4.72 (q, J = 6.8 Hz, 1H), 6.86 (d, J = 9.2 Hz, 2H), 6.94 (d, J = 9.2 Hz, 2H), 7.56 (s, 2H), 8.07 (d, J = 6 Hz, 2H), 8.11 (s, 1H), 8.44 (s, 1H), 8.81 (d, J = 6 Hz, 2H); ^{13}C NMR (CDCl$_3$, 100 MHz) δ 18.8, 55.8, 76.6, 94.6, 111.1, 112.3, 115.1, 117.4, 119.5, 121.2, 134.3, 134.7, 142.4, 148.0,

150.9, 155.2, 161.7, 170.8; ESI-HRMS for $C_{22}H_{20}N_3O_4$ (M+H)$^+$ calcd. 390.1454 found 390.1457.

2-(3-chlorophenoxy)-*N*-(2-(pyridine-4-yl)benzo[d]oxazol-5-yl)propionamide (45): 73%; white solid; ^{1}H NMR (CDCl$_3$, 400 MHz) δ 1.68 (d, *J* = 6.8 Hz, 3H), 4.82 (q, *J* = 6.8 Hz, 1H), 6.86 – 6.89 (m, 1H), 7.02 (d, *J* = 7.6 Hz, 2H), 7.23 – 7.27 (m, 1H), 7.51 – 7.57 (m, 2H), 8.05 (d, *J* = 5.2 Hz, 2H), 8.09 (s, 1H), 8.37 (s, 1H), 8.81 (s, 2H); ^{13}C NMR (CDCl$_3$, 100 MHz) δ 18.7, 75.8, 111.1, 112.5, 113.8, 116.8, 119.6, 121.2, 123.0, 130.9, 134.2, 134.5, 135.5, 142.4, 148.1, 150.9, 157.4, 161.7, 170.0; ESIHRMS for $C_{21}H_{17}N_3O_3Cl$ (M+H)$^+$ calcd. 394.0958, found 394.0959.

2-(2,3-dichlorophenoxy)-*N*-(2-(pyridine-4-yl)benzo[d]oxazol-5-yl)propionamide (46): 71%; white solid; ^{1}H NMR (CDCl$_3$, 400 MHz) δ 1.77 (d, *J* = 6.8 Hz, 3H), 4.91 (q, *J* = 6.8 Hz, 1H), 6.93 (dd, J_1 = 6.6 Hz, J_2 = 2.8 Hz, 1H), 7.20 – 7.23 (m, 2H), 7.60 (d, *J* = 1.2 Hz, 2H), 8.08 (d, *J* = 4.4 Hz, 2H), 8.18 (s, 1H), 8.83 (s, 3H); ^{13}C NMR (CDCl$_3$, 100 MHz) δ 18.3, 76.6, 111.0, 111.8, 113.0, 119.0, 120.9, 122.7, 124.1, 127.8, 134.1, 134.3, 134.5, 142.2, 147.8, 150.7, 153.5, 161.5, 168.9; ESI-HRMS for $C_{21}H_{16}N_3O_3Cl_2$ (M+H)$_+$ calcd. 428.0569, found 428.0569.

2-(2,6-dichlorophenoxy)-*N*-(2-(pyridine-4-yl)benzo[d]oxazol-5-yl)propionamide (47): 67%; white solid; ^{1}H NMR (CDCl$_3$, 400 MHz) δ 1.61 (d, *J* = 6.8 Hz, 3H), 5.11 (q, *J* = 6.8 Hz, 1H), 7.09 (t, *J* = 7.6 Hz, 1H), 7.37 (d, *J* = 8.4 Hz, 2H), 7.60 (d, *J* = 8.8 Hz, 1H), 7.18 (dd, J_1 = 8.8 Hz, J_2 = 1.6 Hz, 1H), 8.08 (d, *J* = 5.2 Hz, 2H), 8.20 (s, 1H), 8.82 (d, *J* = 5.2 Hz, 2H), 8.99 (s, 1H); ^{13}C NMR (CDCl$_3$, 100 MHz) δ 18.2, 79.5, 111.1, 112.1, 119.4, 121.2, 126.1, 129.5, 129.6, 134.3, 135.0, 142.4, 148.0, 148.7, 150.9, 169.5, 195.9; ESI-HRMS for $C_{21}H_{16}N_3O_3Cl_2$ (M+H)$^+$ calcd. 428.0569, found 428.0567.

2-(naphthalene-1-yloxy)-*N*-(2-(pyridine-4-yl)benzo[d]oxazol-5-yl)propionamide (48): 73%; white solid; ^{1}H NMR (CDCl$_3$, 400 MHz) δ 1.84 (d, *J* = 6.4 Hz, 3H), 5.04 (q, *J* = 6.8 Hz, 1H), 6.92 (d, *J* = 7.6 Hz, 1H), 7.39 (t, *J* = 8 Hz, 1H), 7.61 – 7.48 (m, 5H), 7.89 – 7.86 (m,1H), 8.05 – 8.08 (m, 3H), 8.33 – 8.36 (m, 1H), 8.41 (s, 1H), 8.80 (s, 2H); ^{13}C NMR (CDCl$_3$, 100 MHz) δ 19.1, 76.2, 107.3, 111.1, 112.4, 119.6, 121.21, 121.25, 121.5, 122.4, 125.8, 126.0, 126.1, 127.0, 128.1, 134.2, 134.6, 134.9, 142.4, 148.0, 150.9, 152.6, 170.6; ESI-HRMS for $C_{25}H_{20}N_3O_3$ (M+H)$^+$ calcd. 410.1505, found 410.1508.

2-(4-chloronaphthalen-1-yloxy)-*N*-(2-(pyridin-4-yl)benzo[d]oxazol-5-yl)propionamide (49): 68%; white solid. ^{1}H NMR (CDCl$_3$, 400 MHz) δ 1.83 (d, *J* = 6.8 Hz, 3H), 5.0 (q, *J* = 6.8 Hz, 1H), 6.84 (d, *J* = 8.4 Hz, 1H), 7.46 – 7.50 (m, 2H), 7.54 (d, *J* = 8.8 Hz, 1H), 7.63 – 7.71 (m, 2H), 8.04 – 8.07 (m, 3H), 8.27 (d, *J* = 8 Hz, 1H), 8.36 (d, *J* = 8 Hz, 2H), 8.81 (d, *J* = 4 Hz, 2H); ^{13}C NMR (CDCl$_3$, 100 MHz) δ 19.0, 76.5, 107.3, 111.1, 112.5, 119.6, 121.1, 122.0, 124.9, 125.5, 125.9, 126.9, 128.1, 131.8, 134.2, 134.4, 134.4, 134.7, 142.4, 148.1, 150.9, 151.7, 161.8, 170.3; ESI-HRMS for $C_{25}H_{19}N_3O_3Cl$ (M+H)$^+$ calcd. 444.1115, found 444.1119.

3-methyl-2-(naphthalene-1-yloxy)-*N*-(2-(pyridine-4-yl)benzo[d]oxazol-5-yl)butanamide (52): 67%; white solid; ^{1}H NMR (CDCl$_3$, 400 MHz) δ 1.18 (d, *J* = 6.8 Hz, 3H), 1.25 (d, *J* = 6.8 Hz, 3H), 2.51 – 2.59 (m, 1H), 4.69 (d, *J* = 4 Hz, 1H), 6.84 (d, *J* = 7.6 Hz, 1H), 7.31 (t, *J* = 8 Hz, 1H), 7.37 – 7.47 (m, 3H), 7.51 – 7.54 (m, 2H), 7.80 (t, *J* = 6.4 Hz, 1H), 7.95 – 7.97 (m, 3H), 8.34 (d, *J* = 5.6 Hz, 2H), 8.72 (d, *J* = 5.2 Hz, 2H); ^{13}C NMR (CDCl$_3$, 100 MHz) δ 17.5, 19.6, 32.5, 84.5, 106.7, 111.0, 112.7, 119.9, 121.1, 121.5, 122.1, 125.7, 126.0, 127.0, 128.1, 134.2, 134.4, 134.8, 142.2, 148.0, 150.7, 153.5, 161.6, 169.8; ESI-HRMS for $C_{27}H_{24}N_3O_3$ (M+H)$^+$ calcd. 438.1818, found 438.1822.

(*R*)-2-(naphthalene-1-yloxy))-*N*-(2-(pyridine-4-yl)benzo[d]oxazol-5-yl)propionamide (53): 76%; white solid; ^{1}H NMR (CDCl$_3$, 400 MHz) δ 1.83 (d, *J* = 6.8 Hz, 3H), 5.03 (q, *J* = 6.8 Hz, 1H), 6.91 (d, *J* = 7.6 Hz, 1H), 7.38 (t, *J* = 8 Hz, 1H), 7.50 – 7.58 (m, 5H), 7.85 – 7.87 (m, 1H), 8.03 – 8.07 (m, 3H), 8.34 (t, *J* = 2.8 Hz, 1H), 8.47 (s, 1H), 8.80 (bs, 2H); ^{13}C NMR (CDCl$_3$, 100 MHz) δ 19.1, 67.3, 76.2, 107.3, 111.1, 112.4, 119.6, 121.2, 121.5, 122.4, 125.8, 126.0, 126.1, 127.0, 128.1, 134.3, 134.6, 134.9, 142.3, 148.0, 150.9, 152.6, 161.7, 170.6; ESI-HRMS for C$_{25}$H$_{20}$N$_3$O$_3$ (M+H)$^+$ calcd. 410.1505, found 410.1508, Chiral purity (% ee 98.1, t$_R$=22.87).

(*S*)-2-(naphthalene-1-yloxy))-*N*-(2-(pyridine-4-yl)benzo[d]oxazol-5-yl)propionamide (54): 71%; white solid; ^{1}H NMR (CDCl$_3$, 400 MHz) δ 1.78 (d, *J* = 6.8 Hz, 3H), 4.96 (q, *J* = 6.8 Hz, 1H), 6.85 (d, *J* = 7.6 Hz, 1H), 7.30 (t, *J* = 8 Hz, 1H), 7.50 – 7.42 (m, 5H), 7.77 – 7.79 (m, 1H), 7.92 (dd, *J$_1$* = 4.4 Hz, *J$_2$* = 1.6 Hz, 2H), 8.02 (s, 1H), 8.26 – 8.23 (m, 1H), 8.60 (s, 1H), 8.70 (d, *J* = 4.4 Hz, 2H); ^{13}C NMR (CDCl$_3$, 100 MHz) δ 19.1, 76.2, 107.2, 111.0, 112.5, 119.7, 121.1, 121.5, 122.3, 125.0, 125.8, 126.0, 126.9, 128.0, 134.1, 134.7, 134.8, 142.2, 147.9, 150.8, 152.7, 161.6, 170.7; ESI-HRMS for C$_{25}$H$_{20}$N$_3$O$_3$ (M+H)$^+$ calcd. 410.1505, found 410.1507, Chiral purity (% ee 98.9, t$_R$=12.08).

(*S*)-2-(2-chloro-3-(trifluoromethyl)phenoxy)-*N*-(2-(pyridine-4-yl)benzo[d]oxazol-5-yl)propionamide (56): 70%; cream colored solid; ^{1}H NMR (CDCl$_3$, 400 MHz) δ 1.78 (d, *J* = 6.8 Hz, 3H), 4.94 (q, *J* = 6.4 Hz, 1H), 7.21 (d, *J* = 7.6 Hz, 1H), 7.37 – 7.44 (m, 2H), 7.59 (s, 2H), 8.07 (d, *J* = 5.2 Hz 2H), 8.19 (s, 1H), 8.82 (d, *J* = 5.6 Hz, 3H); ^{13}C NMR (CDCl$_3$, 100 MHz) δ 18.5, 76.9, 111.2, 112.1, 118.4, 119.2, 121.1, 122.3, 124.0, 130.4, 134.2, 134.6, 142.4, 148.0, 150.9, 153.5, 161.8, 168.9; ESI-HRMS for C$_{22}$H$_{16}$N$_3$O$_3$ClF$_3$ (M+H)$^+$ calcd. 462.0832, found 462.0834, Chiral purity (% ee 99.4, t$_R$=11.83).

(*S*)-2-(2-chloro-3-nitrophenoxy)-*N*-(2-(pyridine-4-yl)benzo[d]oxazol-5-yl)propionamide (57): 77%; cream colored solid; ^{1}H NMR (CDCl$_3$, 400 MHz) δ 1.80 (d, *J* = 6.8 Hz, 3H), 4.97 (q, *J* = 6.8 Hz, 1H), 7.24 (d, *J* = 8.4 Hz, 1H), 7.44 (t, *J* = 8.4 Hz, 1H), 7.53 – 7.62 (m, 3H), 8.07 – 8.09 (m, 2H), 8.20 (s, 1H), 8.68 (s, 1H), 8.82 – 8.84 9m, 2H); ^{13}C NMR (CDCl$_3$, 100 MHz) δ 18.5, 76.9, 111.3, 112.2, 117.2, 118.0, 118.7, 119.3, 121.2, 128.4, 134.2, 134.4, 142.4, 148.1, 149.9, 150.9, 153.7, 161.9, 168.6; ESI-HRMS for C$_{21}$H$_{16}$N$_4$O$_5$Cl (M+H)$^+$ calcd. 439.0809, found 439.0805, Chiral purity (% ee >99, t$_R$=35.93).

(*S*)-2-(2,3-dimethoxyphenoxy)-*N*-(2-(pyridine-4-yl)benzo[d]oxazol-5-yl)propionamide (58): 79%; white solid; ^{1}H NMR (CDCl$_3$, 400 MHz) δ 1.78 (d, *J* = 6.8 Hz, 3H), 3.89 (s, 3H), 4.01 (s, 3H), 4.78 (q, *J* = 6.8 Hz, 1H), 6.67 – 6.71 (m, 2H), 7.04 (t, *J* = 5.6 Hz, 1H), 7.55 (d, *J* = 8.8 Hz, 1H), 7.68 (dd, *J$_1$* = 9.2 Hz, *J$_2$* = 2.4 Hz, 1H), 8.07 (dd, *J$_1$* = 4.4 Hz, *J$_2$* = 1.6 Hz, 2H), 8.20 (d, *J* = 2 Hz, 1H), 8.82 (dd, *J$_1$* = 4.4 Hz, *J$_2$* = 1.2 Hz, 2H), 9.58 (s, 1H); ^{13}C NMR (CDCl$_3$, 100 MHz) δ 20.5, 57.0, 62.5, 80.3, 108.3, 111.4, 111.8, 112.7, 120.1, 122.0, 125.7, 135.3, 136.4, 140.4, 143.1, 148.6, 151.7, 152.8, 154.9, 162.4, 171.4; ESI-HRMS for C$_{23}$H$_{22}$N$_3$O$_5$ (M+H)$^+$ calcd. 420.1559, found 420.1557, Chiral purity (% ee >99, t$_R$=17.41).

2-(2,4-dichlorophenoxy)-*N*-(2-(phenylbenzo[d]oxazol-5-yl)propionamide (59): 73%; white solid; ^{1}H NMR (CDCl$_3$, 400 MHz) δ 1.74 (d, *J* = 6.8 Hz, 3H), 4.84 (q, *J* = 6.8 Hz, 1H), 6.94 (d, *J* = 8.8 Hz, 1H), 7.23 (dd, *J$_1$* = 8.8 Hz, *J$_2$* = 2.4 Hz, 1H), 7.44 (d, *J* = 2.4 Hz, 1H), 7.54 – 7.51 (m,4H), 7.56 (d, *J* = 2 Hz, 1H), 7.59 (d, *J* = 2 Hz, 1H), 8.05 (d, *J* = 1.6 Hz, 1H), 8.24 (dd, *J* = 8 Hz, 2H), 8.75 (s, 1H); ^{13}C NMR (CDCl$_3$, 100 MHz) δ 18.6, 76.9, 110.8, 111.6, 116.4, 118.0, 124.7, 127.1, 127.8, 128.0, 128.4, 129.1, 130.6, 131.9, 134.2, 142.8, 148.0, 151.3, 164.2, 169.1; ESI-HRMS for C$_{22}$H$_{17}$N$_2$O$_3$Cl$_2$ (M+H)$^+$ calcd. 427.0616 found 427.0619.

(*S*)-2-(2,3-dichlorophenoxy)-*N*-(2-(thiazol-5-yl)benzo[d]oxazol-5-yl)propionamide (62):
76%; white solid; ^{1}H NMR (CDCl$_3$, 400 MHz) δ 1.76 (d, *J* = 6.8 Hz, 3H), 4.89 (q, *J* = 6.8
Hz, 1H), 6.92 (dd, *J*$_1$ = 7.2 Hz, *J*$_2$ = 2.4 Hz, 1H), 7.17 – 7.22 (m, 2H), 7.55 (q, *J* = 8.8 Hz,
2H), 8.09 (s, 1H), 8.64 (s, 1H), 8.81 (s, 1H); ^{13}C NMR (CDCl$_3$, 100 MHz) δ 18.6, 76.9,
110.9, 111.6, 113.2, 118.6, 120.5, 122.9, 124.3, 125.7, 128.1, 134.7, 142.4, 145.7, 147.6,
153.7, 156.4, 158.0, 169.1; ESI-HRMS for C$_{19}$H$_{14}$N$_3$O$_3$SCl$_2$ (M+H)$^+$ calcd. 434.0133,
found 434.0136, Chiral purity (% ee 99.1, t$_R$=15.5).

(*S*)-2-(naphthalene-1-yloxy)-*N*-(2-(thiazol-5-yl)benzo[d]oxazol-5-yl)propionamide (63):
78%; white solid; ^{1}H NMR (CDCl$_3$, 400 MHz) δ 1.81 (d, *J* = 6.8 Hz, 3H), 5.01 (q, *J* = 6.4
Hz, 1H), 6.89 (d, *J* = 7.6 Hz, 1H), 7.35 (t, *J* = 7.6 Hz, 1H), 7.45 – 7.54 (m, 5H), 7.82 (t, *J* =
4.8 Hz, 1H), 7.96 (s, 1H), 8.29 (d, *J* = 5.2 Hz, 1H), 8.55 (d, *J* = 21.6 Hz, 2H), 8.91 (s,
1H); ^{13}C NMR (CDCl$_3$, 100 MHz) δ 19.1, 76.2, 107.3, 110.7, 112.0, 119.0, 121.5, 122.3,
125.6, 125.8, 126.0, 126.1, 127.0, 128.0, 134.6, 134.8, 142.2, 145.6, 147.6, 152.6, 156.4,
157.8, 170.6; ESI-HRMS for C$_{23}$H$_{18}$N$_3$O$_3$S (M+H)$^+$ calcd. 416.1069, found 416.1075,
Chiral purity (% ee 98.7, t$_R$=12.53).

**2-(4-chloronaphthalen-1-yloxy)-*N*-(2-(thiazol-5-yl)benzo[d]oxazol-5-yl)propionamide
(64):** 64%; white solid; ^{1}H NMR (CDCl$_3$, 400 MHz) δ 1.82 (d, *J* = 6.8 Hz, 3H), 4.99 (q, *J* =
6.8 Hz, 1H), 6.83 (d, *J* = 8.4 Hz, 1H), 7.44 – 7.50 (m, 3H), 7.62 – 7.71 (m, 2H), 7.98 (d, *J* =
2 Hz, 1H), 8.25 – 8.37 (m, 3H), 8.62 (s, 1H), 8.96 (s, 1H); ^{13}C NMR (CDCl3, 100 MHz) δ
19.1, 76.6, 107.4, 110.9, 112.1, 119.0, 122.0, 125.0, 125.6, 126.0, 126.9, 127.0, 128.2,
131.8, 134.5, 142.4, 145.8, 147.8, 151.7, 156.5, 161.8, 166.4, 170.3; ESI-HRMS for
C$_{23}$H$_{17}$N$_3$O$_3$SCl (M+H)$^+$ calcd. 450.0679, found 450.0680.

(*S*)-2-(2,3-dichlorophenoxy)-*N*-(2-(thiazol-2-yl)benzo[d]oxazol-5-yl)propionamide (65):
69%; white solid; ^{1}H NMR (CDCl$_3$, 400 MHz) δ 1.72 (d, *J* = 6.8 Hz, 3H), 4.85 (q, *J* = 6.8
Hz, 1H), 6.89 (dd, *J*$_1$ = 8 Hz, *J*$_2$ = 2 Hz, 1H), 7.12 – 7.18 (m, 2H), 7.55 (bs, 2H), 7.59 (d, *J* =
2.8 Hz, 1H), 8.03 (d, *J* = 3.2 Hz, 1H), 8.14 (d, *J* = 1.2 Hz, 1H); ^{13}C NMR (CDCl$_3$, 100
MHz) δ 18.6, 77.0, 111.5, 112.0, 113.2, 119.5, 122.9, 123.5, 124.3, 128.0, 134.5, 134.9,
142.0, 145.3, 147.8, 153.7, 154.7, 158.0, 169.2; ESI-HRMS for C$_{19}$H$_{14}$N$_3$O$_3$SCl$_2$ (M+H)$^+$
calcd. 434.0133, found 434.0132, Chiral purity (% ee >99, t$_R$=12.88).

(*N*-(2-(1*H*-pyrrol-2-yl)benzo[d]oxazol-5-yl)2-(naphthalene-1-yloxy)propionamide (66):
70%; white solid; ^{1}H NMR (CDCl$_3$, 400 MHz) δ 1.82 (d, *J* = 6.8 Hz, 3H), 5.02 (q, *J* = 6.4
Hz, 1H), 6.36 (dd, *J*$_1$ = 2.4 Hz, *J*$_2$ = 6 Hz, 1H), 6.91 (d, *J* = 8 Hz, 1H), 7.06 (d, *J* = 1.6 Hz,
2H), 7.32 – 7.43 (m,3H), 7.52 – 7.60 (m, 3H), 7.85 – 7.89 (m, 2H), 8.34 (d, *J* = 12 Hz, 2H),
9.87 (d, *J* = 1.6 Hz, 1H); ^{13}C NMR (CDCl$_3$, 100 MHz) δ 19.1, 76.2, 107.3, 110.4, 111.0,
111.1, 113.7, 117.5, 119.5, 120.5, 121.5, 122.3, 123.6, 126.0, 126.0, 126.1, 127.0, 128.1,
134.1, 134.9, 142.0, 147.2, 152.6, 159.0, 170.5; ESI-HRMS for C$_{24}$H$_{20}$N$_3$O$_3$ (M+H)$^+$ calcd.
398.1505, found 398.1509.

2-(naphthalene-1-yloxy)-*N*-(2-(pyrimidin-2-yl)benzo[d]oxazol-5-yl)propionamide (67):
63%; white solid; ^{1}H NMR (CDCl$_3$, 400 MHz) δ 1.83 (d, *J* = 6.8 Hz, 3H), 5.04 (q, *J* = 6.8
Hz, 1H), 6.93 (d, *J* = 7.6 Hz, 1H), 7.39 (t, *J* = 8.4 Hz, 1H), 7.61 – 7.53 (m, 4H), 7.88 – 7.86
(m, 1H), 8.09 (s, 1H), 8.34 (d, *J* = 7.2 Hz, 1H), 8.44 (s, 1H), 8.99 (d, *J* = 4.8 Hz, 2H); ^{13}C
NMR (CDCl$_3$, 100 MHz) δ 19.1, 76.4, 107.5, 111.7, 111.7, 113.1, 120.5, 121.5, 122.2,
122.4, 125.9, 126.0, 126.1, 127.0, 128.1, 134.8, 134.9, 142.2, 148.4, 152.7, 155.2, 158.2,
170.7; ESI-HRMS for C$_{24}$H$_{19}$N$_4$O$_3$ (M+H)$^+$ calcd. 411.1457, found 411.1460.

**(*S*)-*N*-(7-chloro-2-(pyridin-4-yl)benzo[d]oxazol-5-yl)-2-(2,3-
dichlorophenoxy)propionamide (68):** 68%; white solid; ^{1}H NMR (CDCl$_3$, 400 MHz) δ

1.73 (d, J = 6.8 Hz, 3H), 4.87 (q, J = 6.8 Hz, 1H), 6.90 (dd, J_1 = 6.4 Hz, J_2 = 3.2 Hz, 1H), 7.18 – 7.23 (m, 2H), 7.75 (d, J = 2 Hz, 1H), 7.97 (d, J = 1.6 Hz, 1H), 8.08 (d, J = 5.2 Hz, 2H), 8.82 (d, J = 8 Hz, 3H); ^{13}C NMR (CDCl$_3$, 100 MHz) δ 18.5, 77.0, 110.4, 113.3, 116.5, 119.2, 121.3, 124.5, 128.1, 133.7, 134.6, 135.3, 143.2, 144.8, 150.9, 153.6, 162.1, 162.6, 169.3; ESI-HRMS for C$_{21}$H$_{15}$N$_3$O$_3$Cl$_3$ (M+H)$^+$ calcd. 462.0179 found 462.0182, Chiral purity (% ee >99, t$_R$= 4.52).

2-methyl-3-phenyl-*N*-(2-(pyridine-4-yl)benzo[d]oxazol-5-yl)propionamide (69): 75%; white solid; ^{1}H NMR (CDCl$_3$, 400 MHz) δ 1.29 (d, J = 6 Hz, 3H), 2.63 (q, J = 6.4 Hz, 1H), 2.77 (dd, J_1 = 16 Hz, J_2 = 5.6 Hz, 1H), 3.02 (dd, J_1 = 16 Hz, J_2= 9.2 Hz, 1H), 7.17 – 7.25 (m, 5H), 7.34 – 7.44 (m, 3H), 7.75 (s, 1H), 7.99 (d, J = 4 Hz, 2H), 8.75 (s, 2H); ^{13}C NMR (CDCl$_3$, 100 MHz) δ 18.0, 40.9, 44.9, 110.9, 112.5, 120.0, 121.2, 126.7, 128.8, 129.1, 134.4, 135.3, 139.8, 142.1, 147.8, 150.8, 174.3; ESI-HRMS for C$_{22}$H$_{20}$N$_3$O$_2$ (M+H)$^+$ calcd. 358.1556 found 358.1556.

2-phenyl-*N*-(2-(pyridine-4-yl) benzo[d]oxazol-5-yl)propionamide (70): 77%; ^{1}H NMR (CDCl$_3$, 400 MHz) δ 1.61 (d, J = 7.2 Hz, 3H), 3.74 (q, J = 7.2 Hz, 1H), 7.17 (s, 1H), 7.23 (s, 1H), 7.29 – 7.32 (m, 1H), 7.37 – 7.41 (m, 4H), 7.47 (d, J = 8.8 Hz, 1H), 7.91 (d, J = 1.6 Hz, 1H), 8.01 (dd, J_1 = 1.6 Hz, J_2 = 1.2 Hz, 2H), 8.77 (d, J = 5.6 Hz, 2H); ^{13}C NMR (CDCl$_3$, 100 MHz) δ 18.8, 48.3, 110.9, 112.1, 119.4, 121.1, 127.92, 127.94, 129.4, 134.3, 135.4, 140.9, 142.3, 147.8, 150.9, 161.6, 172.5; ESI-HRMS for C$_{21}$H$_{18}$N$_3$O$_2$ (M+H)$^+$ calcd. 344.1399, found 344.1400.

(*S*)-2-phenyl-*N*-(2-(pyridine-4-yl)benzo[d]oxazol-5-yl)propionamide (71): 77%; ^{1}H NMR (CDCl$_3$, 400 MHz) δ 1.52 (d, J = 7.2 Hz, 3H), 3.67 (q, J = 7.2 Hz, 1H), 7.15 (t, J = 8.4Hz, 1H), 7.21 – 7.35 (m, 5H), 7.69 (s, 1H), 7.83 (s, 1H), 7.91 (d, J = 5.6 Hz, 2H), 8.68 (d, J = 5.2 Hz, 2H); ^{13}C NMR (CDCl$_3$, 100 MHz) δ 18.9, 31.1, 42.7, 48.0, 110.8, 112.2, 119.7, 120.5, 121.1, 127.7, 127.8, 128.1, 129.3, 134.3, 135.6, 141.1, 142.1, 147.7, 148.4, 149.1, 150.8, 161.4, 172.9; ESI-HRMS for C$_{21}$H$_{18}$N$_3$O$_2$ (M+H)$^+$ calcd. 344.1399, found 344.1397, Chiral purity (% ee >99, tR = 8.07 min).

(*R*)-2-phenyl-*N*-(2-(pyridine-4-yl)benzo[d]oxazol-5-yl)propionamide (72): 78%; white solid; ^{1}H NMR (CDCl$_3$, 400 MHz) δ 1.59 (d, J = 7.2 Hz, 3H), 3.76 (q, J = 6.8 Hz, 1H), 7.21 – 7.29 (m, 1H), 7.32 – 7.41 (m, 6H), 7.90 (s, 1H), 7.97 (d, J = 4.8 Hz, 3H), 8.74 (s, 2H); ^{13}C NMR (CDCl$_3$, 100 MHz) δ 18.9, 48.0, 110.8, 112.3, 119.8, 121.2, 127.7, 127.8, 129.2, 134.3, 135.6, 141.1, 142.1, 147.7, 150.7, 161.4, 172.9; ESI-HRMS for C$_{21}$H$_{18}$N$_3$O$_2$ (M+H)$^+$ calcd. 344.1399, found 344.1393, Chiral purity (% ee 99, t$_R$=11.29 min).

2-(2,3-dichlorophenylamino)-*N*-(2-(pyridine-4-yl)benzo[d]oxazol-5-yl)propionamide (73): 71%; ^{1}H NMR (CDCl$_3$, 400 MHz) δ 1.72 (d, J = 6.8 Hz, 3H), 3.95 (dq, J_1 = 7.2 Hz, J_2 = 3.2 Hz, 1H), 4.79 (d, J = 2.8 Hz, 1H), 6.56 (d, J = 8.4 Hz, 1H), 6.96 (d, J = 8 Hz, 1H), 7.09 (t, J = 8 Hz, 1H), 7.46 (dd, J_1 = 9.2 Hz, J_2 = 2 Hz, 1H), 7.54 (d, J = 8.4 Hz, 1H), 8.06 (d, J = 4 Hz, 2H), 8.09 (d, J = 1.6 Hz, 1H), 8.56 (s, 1H), 8.8 (bs, 2H); ^{13}C NMR (CDCl$_3$, 100 MHz) δ 20.0, 56.4, 110.8, 111.1, 112.4, 118.6, 119.6, 120.9, 121.2, 128.4, 133.5, 134.3, 134.7, 142.4, 144.1, 148.0, 150.9, 161.7, 171.7; ESI-HRMS for C$_{21}$H$_{17}$N$_4$O$_2$Cl$_2$ (M+H)$^+$ calcd. 427.0729 found 427.0724.

Preparation of (*S*)-*N*-methyl-2-(naphthalen-1-yloxy)-*N*-(2-(thiazol-5-yl)benzo[d]oxazol-5-yl)propanamide (9, R$_1$ = 5-thiazole, R$_2$ = 1-naphthyl, R$_3$= (*S*)-Me, Y = O, X = H)—A solution of **63** (30 mg, 0.072 mmol) in 2 mL anhydrous THF was added drop-wise to a suspension of sodium hydride (60% in mineral oil, 1.89 mg, 0.079 mmol) in anhydrous THF (3 mL) under a nitrogen atmosphere at 0 °C. The resulting mixture

was stirred for 30 min at room temperature. The mixture was cooled to 0 °C and then MeI (11.2 mg, 0.079 mmol) was added. The reaction mixture was stirred for 1 h at room temperature. The reaction mixture was quenched with a few drops of water and extracted with DCM. The organic layers were washed with brine, dried over anhydrous $MgSO_4$, filtered, and concentrated. The residue was purified by silica gel column chromatography using ethyl acetate/*n*-hexane (40:60) to yield **9** (15 mg, 48%) as a white solid. ^{1}H NMR (CDCl$_3$, 400 MHz) δ 1.62 (d, *J* = 6.4 Hz, 3H), 3.34 (s, 3H), 4.92 (q, *J* = 6.4 Hz, 1H), 6.49 (d, *J* = 7.6 Hz, 1H), 7.03 (d, *J* = 8.4 Hz, 1H), 7.19 – 7.39 (m, 6H), 7.69 (d, *J* = 8 Hz, 1H), 7.90 (d, *J* = 8.4 Hz, 1H), 8.61 (s, 1H), 8.61 (s, 1H), 8.98 (s, 1H); ^{13}C NMR (CDCl3, 100 MHz) δ 18.7, 39.0, 72.6, 105.9, 111.4, 119.0, 121.3, 122.3, 125.2, 125.29, 125.3, 125.5, 126.0, 126.5, 127.4, 134.7, 140.0, 142.6, 146.0, 149.7, 153.0, 156.9, 158.4, 171.3; ESI-HRMS for $C_{24}H_{20}N_3O_3S$ (M+H)+ calcd. 430.1225, found 430.1222, Chiral purity (% ee >99, tR=12.2 min.

Preparation of (*S*)-2-((2,3-dichlorophenyl)amino)propionoic acid (11)—A mixture of **10** (163 mg, 1.82 mmol), 2,3-dichloro iodobenzene (500 mg, 1.83 mmol), Cs2CO3 (1.19 gr, 3.65 mmol), and CuI (69.7 mg, 0.36 mmol) in DMF (3 mL) under a nitrogen atmosphere was heated at 90 °C for 48 h. The mixture was allowed to cool to room temperature and then diluted with water and the pH was adjusted to 3 to 5 by the addition of concentrated HCl. The mixture was extracted with DCM. The organic layers were washed with brine, dried over anhydrous MgSO4, filtered, and concentrated. The residue was purified by silica gel flash column chromatography using ethyl acetate/*n*-hexane (50:50) to afforded **11** (240 mg, 57%) as a brown solid. ^{1}H NMR (CDCl$_3$, 400 MHz) δ 1.60 (d, *J* = 7.2 Hz, 3H), 4.17 (q, *J* = 7.2 Hz, 1H), 6.48 (d, *J* = 8 Hz, 1H), 6.85 (d, *J* = 8 Hz, 1H), 7.05 (t, *J* = 8.4 Hz, 1H).

Synthesis of (*S*)-2-(2,3-dichlorophenylamino)-*N*-(2-(pyridine-4-yl)benzo[d]oxazol-5-yl) propionamide (15a)—The general procedure for **8** was followed using **11** and **4** to produce **15a**; 70%; brown solid; ^{1}H NMR (CDCl$_3$, 400 MHz) δ 1.72 (d, *J* = 6.8 Hz, 3H), 3.95 (dq, J$_1$ = 7.2 Hz, J$_2$ = 3.2 Hz, 1H), 4.79 (d, *J* = 2.8 Hz, 1H), 6.56 (d, *J* = 8.0 Hz, 1H), 6.96 (d, *J* = 8 Hz, 1H), 7.09 (t, *J* = 8 Hz, 1H), 7.47 (d, *J* = 8.4 Hz, 1H), 7.54 (d, *J* = 8.8 Hz, 1H), 8.08 (bd, 3H), 8.56 (s, 1H), 8.8 (bs, 2H); ^{13}C NMR (CDCl$_3$, 100 MHz) δ 19.9, 56.35, 110.7, 111.0, 112.5, 118.5, 119.7, 120.7, 121.2, 128.3, 133.5, 134.3, 134.8, 142.3, 144.1, 148.0, 150.8, 161.6, 171.9; ESI-HRMS for $C_{21}H_{17}N_4O_2Cl_2$ (M+H)$^+$ calcd. 427.0729 found 427.0731, Chiral purity (% ee 90.5, t$_R$ = 20.4 min).

Preparation of (*S*)-methyl 2-(naphthalen-1-ylamino)propanoate (13)—Into a dry round bottom flask equipped with a stir bar was added L-alanine methyl ester hydrochloride (500 mg, 3.58 mmol), 1-naphthalene boronic acid (1000 mg, 5.81 mmol), Cu(OAc)$_2$ (715 mg, 3.93 mmol), and 4 Å molecular sieves (1.34 g). The flask was sealed with a septum, evacuated and back filled with oxygen. Triethylamine (0.92 mL) and dry DCM (30 mL) were added. The reaction mixture was stirred at room temperature for 48 h. The reaction mixture was quenched with 13 mL 2M NH$_3$ in methanol. The volatiles were removed in vacuo and the resulting crude oil was purified by silica gel flash chromatography using ethyl acetate/*n*-hexane (10:90) to give **13** (280 mg, 34%) as a brown viscous oil. ^{1}H NMR (CDCl$_3$, 400 MHz) δ 1.27 (t, *J* = 6.8 Hz, 3H), 1.61 (d, *J* = 6.8 H, 3H), 4.23 (q, *J* = 6.8 Hz, 2H), 4.31 (q, *J* = 6.4 Hz, 1H), 4.98 (bs, NH), 6.55 (d, *J* = 7.2 Hz, 1H), 7.27–7.35 (m, 2H), 7.45–7.49 (m, 2H), 7.78–7.81 (m, 1H), 7.90–7.93 (m, 1H).

Preparation of *N*-1-naphthalenyl L-alanine (14)—Ester **13** (40 mg, 0.174 mmol) was dissolved in methanol (1mL) and 1M NaOH in aqueous solution (0.18 mmol, 1.1 eq) was added drop-wise. The reaction mixture was stirred at room temperature for 12 h and then

concentrated. The residue was dissolved in DCM and then extracted with 10% aqueous Na_2CO_3 solution. The aqueous layer was acidified with 1M HCl. The precipitate was collected and washed with DCM. The solid was purified by silica gel flash column chromatography using ethyl acetate/*n*-hexane (40:70) to give **14** (25 mg, 67%) as a brown solid. ^{1}H NMR (CDCl$_3$, 400 MHz) δ 1.60 (d, *J* = 6.8 Hz, 3H), 4.24 (q, *J* = 6.8 Hz, 1H), 6.49 (d, *J1* = 6 Hz, *J2* = 1.6 Hz, 1H), 7.18–7.25 (m, 2H), 7.39–7.41 (m, 2H), 7.72–7.81 (m, 2H).

Synthesis of (*S*)-2-(naphthalen-1-ylamino)-*N*-[2-(pyridin-4-yl)benzo[d]oxazol-5-yl]propionamide (15b)—

The general procedure for **8** was followed using **14** and **4** to produce **15b** (60%) as a brown solid. ^{1}H NMR (CDCl$_3$, 400 MHz) δ 1.79 (d, *J* = 6.8 Hz, 3H), 4.13 (q, *J* = 6.8 Hz, 1H), 4.69 (bs, 1H), 6.66 (d, *J* = 7.2 Hz, 1H), 7.56- 7.32 (m, 6H), 7.87 (d, *J* = 7.2 Hz, 1H), 7.95 (d, J = 8 Hz, 1H), 8.08 (bs, 3H), 8.79 (bs, 3H); ^{13}C NMR (CDCl$_3$, 100 MHz) δ 20.2, 56.4, 106.9, 110.9, 112.4, 119.6, 12.7, 120.3, 121.1, 123.6, 125.7, 126.3, 126.6, 129.2, 134.3, 134.4, 135.0, 141.4, 142.3, 147.9, 150.9, 161.6, 172.4; ESI-HRMS for $C_{25}H_{20}N_4O_2$ (M+H)$_+$ calcd. 409.1586 found 409.1668, Chiral purity (% ee 97, t_R = 36.4 min).

Preparation of 2-(2,3-dichlorophenyl)acetyl chloride (17)—

2,3-Dichlorophenylacetic acid (**16**, 500 mg, 2.43 mmol) was dissolved in thionyl chloride (4 mL) under a nitrogen atmosphere at 0 °C. The reaction mixture was heated at 90 °C for 2 h. The excess thionyl chloride was removed in vacuo to afford **17** as a colorless liquid. This material was used without further purification.

Preparation of (*R*)-4-benzyl-3-(2-(2,3-dichlorophenyl)acetyl)oxazolidin-2-one (19)—

(*R*)-4-benzyloxazolidin-2-one (**18**, 212.6 mg, 1.19 mmol) was dissolved in anhydrous THF (8 mL) under a nitrogen atmosphere. The reaction mixture was cooled to −78 °C and then a 2.5M solution of *n*-butyl lithium in hexanes (0.9 mL, 1.2 mmol) was added drop-wise. After 1 h, **17** (492 mg, 2.4 mmol) was added. The reaction mixture was stirred for 15 min −78 °C. Then the reaction mixture was allowed to warm to 0 °C and stirred for 30 min. The reaction mixture was then quenched with saturated aqueous NH_4Cl solution. The solvent was removed in vacuo, and then the mixture was extracted with DCM. The organic layer was washed with brine, dried over anhydrous $MgSO_4$, filtered, and concentrated. The residue was purified by silica gel column chromatography using EtOAc/*n*-hexane (20:80) to give **19** (350 mg, 80%) as a brown semi-solid. ^{1}H NMR (CDCl$_3$, 400 MHz) δ 2.77 (t, *J* = 12 Hz, 1H), 3.29 (d, *J* = 12.8 Hz, 1H), 4.23 (m,2H), 4.35 (d, *J* = 18.4 Hz, 1H), 4.47 (d, *J* = 18.4 Hz, 1H), 4.67 (m,1H), 7.16–7.30 (m, 7H), 7.40 (dd, J_1 = 4 Hz, J_2 = 2.4 Hz, 1H).

Preparation of (4*R*)-4-benzyl-3-(2-(2,3-dichlorophenyl)propanoyl)oxazolidin-2-one (20)—

To a solution of **19** (250 mg, 0.686 mmol) in anhydrous THF (10 mL) was added sodium bis(trimethylsilyl)amide (0.61 mL, 0.617 mmol) at −78 °C under a nitrogen atmosphere. After 1 h, methyl iodide (0.192 mL, 3 mmol) was slowly added. The reaction mixture was stirred for 2 h at −78 °C and then allowed to warm to room temperature over 5 h. Reaction mixture was quenched with saturated aqueous NH_4Cl. The mixture was diluted with DCM. The organic layer was washed sequentially with water, saturated sodium sulfite and brine. The organic phase was dried over anhydrous $MgSO_4$, filtered and concentrated. The residue was purified by silica gel chromatography eluting with a linear gradient ranging from 5 to 20% ethyl acetate in *n*-hexane to provide **20** (200 mg, 77%) as a white foam. ^{1}H NMR (CDCl$_3$, 400 MHz) δ 1.56 (d, *J* = 6.8 Hz, 3H), 2.79 (t, *J* = 12.0 Hz, 1H), 3.28 (d, *J* = 13.6 Hz, 1H), 4.09–4.16 (m, 2H), 4.66 (bs, 1H), 5.37 (q, *J* = 6.8 Hz,1 H), 7.19–7.37 (m, 8H).

Preparation of (*R*)-2-(2,3-dichlorophenyl)propionic acid (21)—

To a solution of **20** (160 mg, 0.42 mmol) in THF (5 mL) and water at 0 °C, was added drop-wise a solution of

lithium peroxide [prepared by adding 30% hydrogen peroxide (2.9mL, 2.10 mmol) to lithium hydroxide (17.6 mg, 0.41 mmol) in water (0.679 mL)]. The reaction mixture was stirred for 0 °C for 1 h, and then quenched with saturated aqueous Na_2SO_3 (1.28 mL). The solvent was removed in vacuo. The residue was diluted with water and then extracted with DCM (2 times). The aqueous layer was acidified with concentrated HCl and then extracted with EtOAc (2 times). The EtOAc extracts were combined, washed with brine, dried over anhydrous $MgSO_4$, and concentrated. The residue was purified by silica gel column chromatography using EtOAc/*n*-hexane (40:60) to afforded **21** (80 mg, 87%) as a white solid. ^{1}H NMR (CDCl$_3$, 400 MHz) δ 1.51 (d, J = 7.2 Hz, 3H), 4.27 (q, J = 6.8 Hz, 1H), 7.16–7.24 (m, 2H), 7.37(d, J = 7.6 Hz, 1H).

Synthesis of (*R*)-2-(2,3-dichlorophenyl-*N*-(2-(pyridine-4-yl)benzo[d]oxazol-5-yl)propionamide (22)—The general procedure for **8** using **21** and **4** yielded **22** as a white solid (70%); ^{1}H NMR (CDCl$_3$, 400 MHz) δ 1.61 (d, J = 7.2 Hz, 3H), 4.31 (q, J = 6.8 Hz, 1H), 7.26 (t, J = 8 Hz, 1H), 7.42 – 7.54 (m, 4H), 7.98 (s, 1H), 8.05 (d, J = 4.4 Hz, 2H), 8.80 (d, J = 4 Hz, 2H); ^{13}C NMR (CDCl$_3$, 100 MHz) δ 17.8, 45.0, 111.0, 112.4, 119.7, 121.2, 126.8, 128.2, 129.7, 132.0, 133.7, 134.3, 135.4, 140.9, 142.3, 147.9, 150.8, 161.6, 171.3. ESI-HRMS for $C_{21}H_{15}Cl_2N_3O_2$ (M+H)$^+$ calcd. 412.0620, found 412.0611, Chiral purity (% ee 83, t_R = 1.58 min).

Synthesis of 5-nitro-2-(pyridine-4-yl)-1*H*-benzo[d]imidazole (24)—4-Nitro-1,2-phenylenediamine (**23**, 500 mg, 3.26 mmol) and 4-pyridine carboxaldehyde (419 mg, 3.91 mmol) were dissolved in DMF (10 mL). Disodium metabisulfite (742 mg, 3.91 mmol) was added. The reaction mixture was heated at 120 °C for 24 h under a nitrogen atmosphere. After allowing the mixture to cool to room temperature, volatiles were removed under reduced pressure. The reaction mixture was then diluted with water and extracted from DCM. The organic layer was dried on anhydrous $MgSO_4$, filtered and concentrated. The residue was purified by silica gel column chromatography using MeOH/CHCl$_3$ (5:95) to give **24** (480 mg, 61%) as a red solid. ^{1}H NMR (CDCl$_3$, 400 MHz) 8.7 (d, J = 9.2 Hz, 2H), 8.1 (d, J = 2.4 Hz, 1H), 8.03 (d, J = 8.2 Hz, 2H), 7.92 (dd, J_1 = 8.0 Hz, J_2 = 2.4 Hz, 1H), 7.82 (s, 1H).

Synthesis of 2-(pyridin-4-yl)-1*H*-benzo[d]imidazole-5-amine (25)—Substrate **24** was reduced by hydrogenation using the general procedure described for **4** to yield **25** (64%). ^{1}H NMR (CDCl$_3$, 400 MHz) 8.50 (d, J = 8.2 Hz, 2H), 7.44 (d, J = 8.2 Hz, 2H), 6.70 (dd, J_1 = 8 Hz, J_2 = 2Hz, 1H), 6.20–6.17 (dd, J_1= 8 Hz, J_2 = 2 Hz, 1H), 6.10 (s, 1H), 4.30 (s, 2H).

Preparation of 2-phenoxy-*N*-[2-pyridin-4-yl)-1*H*-benzo[d]imidazole-5-yl]propionamide (26)—To a solution of **25** (50 mg, 0.237 mmol) in anhydrous THF (6 mL) was added 2-phenoxypropionyl chloride (52.5 mg, 0.284 mmol), TEA (36.2 mg, 0.355 mmol), 4-DMAP (2.89 mg, 0.023 mmol) at 0 °C. The reaction mixture was stirred for 30 min at room temperature and quenched with sodium bicarbonate solution. The reaction mixture was diluted with DCM and washed with sodium bicarbonate solution followed by brine solution. The organic layer was dried over anhydrous $MgSO_4$, filtered and concentrated. The residue was purified by silica gel column chromatography using MeOH/CHCl$_3$ (10:90) to furnish **26** (60 mg, 70%) as a brown solid. ^{1}H NMR (CDCl$_3$, 400 MHz) δ 1.68 (d, J = 6.8 Hz, 3H), 4.85 (q, J = 6.4 Hz, 1H), 6.95 – 7.05 (m, 4H), 7.26 – 7.32 (m, 2H), 7.52 (d, J = 8.4 Hz, 1H), 7.86 (d, J = 5.2 Hz, 2H), 8.08 (s, 1H), 8.57 (d, J = 5.2 Hz, 2H), 8.65 (s, 1H); ^{13}C NMR (CDCl$_3$, 100 MHz) δ 18.9, 75.5, 115.9, 117.72, 117.74, 120.8, 122.8, 130.1, 132.8, 137.6, 150.0, 150.3, 156.7, 171.5; ESI-HRMS for $C_{21}H_{16}N_3O_3Cl_2$ (M+H)$_+$ calcd. 428.0569 found 428.0578.

Synthesis of (but-3-yn-2-yloxy)benzene (28)—Phenol (**27**, 422.9 mg, 4.49 mmol) and but-3-yn-2-ol (300 mg, 4.28 mmol) were dissolved in anhydrous THF (10 mL) under a nitrogen atmosphere at 0 °C. Then Ph_3P (1.12 g, 4.26 mmol) was added portion-wise. The reaction mixture was stirred for 10 min and then DEAD (894.6 mg, 5.14 mmol) was slowly added. The resulting solution was heated at 70 °C for 20 h. The reaction mixture was allowed to cool to room temperature and then water was added. The mixture was extracted with DCM. The organic layer was dried over anhydrous $MgSO_4$, filtered, and concentrated. The residue was purified by silica gel flash chromatography using ethyl acetate/*n*-hexane (5:95) providing **28** (450 mg, 69%) as a solid. ^{1}H NMR ($CDCl_3$, 400 MHz) δ 1.67 (d, $J =$ 6.8 Hz, 3H), 2.47 (d, $J = 2$ Hz, 1H), 4.88 (q, $J = 2$ Hz, 1H), 6.97 – 7.03 (m, 3H), 7.28 – 7.32 (m, 2H).

Preparation of 5-azido-2-(thiazol-5-yl)benzo[d]oxazole (29)—A solution of 2-(thiazol-5-yl)benzo[d]oxazol-5-amine (**4**, R_1 = 5-thiazole, X = H, 50 mg, 0.23 mmol) dissolved in 2 mL concentrated HCl:H_2O (1:1) was cooled at −5 °C. Then a solution of sodium nitrite (31.7 mg, 0.459 mmol) dissolved in water (15 mL) was slowly added. The reaction mixture was stirred for 60 min and then neutralized with sodium acetate (37.7 mg, 0.459 mmol). Next, a solution of NaN_3 (29.9 mg, 0.49 mmol) in water (0.5 mL) was slowly added over a 30 min period maintaining a temperature between 0 – 5 °C. After additional stirring for 30 min, the solution was allowed to warm to room temperature and then it was extracted with ethyl acetate. The organic layer was dried over anhydrous $MgSO_4$, filtered and concentrated to yield **29** (50 mg, 89%) as a solid, which was used without further purification.

Preparation of 5-(4-(1-phenoxyethyl)-1*H*-1,2,3-triazol-1-yl)-2-(thiazol-5-yl)benzo[d]oxazole (30)—A mixture of **29** (37 mg, 0.15 mmol) and **28** (20 mg, 0.13 mmol) were dissolved in anhydrous acetonitrile (3 mL) under a nitrogen atmosphere. Then DIPEA (53 mg, 0.40 mmol) was added and the mixture stirred at room temperature for 10 min. Next, CuI (51.7 mg, 0.27 mmol) was added portionwise and then the reaction mixture was stirred for 40 min. The mixture was quenched with aqueous saturated NH_4Cl, diluted with water and extracted with DCM. The organic layer was dried over anhydrous $MgSO_4$, filtered and concentrated. The residue was purified by silica gel column chromatography using ethyl acetate/*n*-hexane (50:50) to furnish **30** (43 mg, 84%) as a solid. ^{1}H NMR ($CDCl_3$, 400 MHz) δ 1.77 (d, $J = 6.4$ Hz, 3H), 5.69 (q, $J = 6.4$ Hz, 1H), 6.90 – 6.97 (m, 3H), 7.22 – 7.24 (m, 2H), 7.66 (d, $J = 8.8$ Hz, 1H), 7.74 (dd, $J_1 = 8$ Hz, $J_2 = 2$ Hz, 1H), 7.90 (s, 1H), 7.99 (d, $J = 2$ Hz, 1H), 8.66 (s, 1H), 8.98 (s, 1H); ^{13}C NMR (Pyridine-d_5, 100 MHz) δ 22.1, 69.5, 112.3, 112.5, 116.6, 119.1, 121.7, 121.8, 125.8, 130.3, 135.3, 143.2, 146.9, 150.5, 151.1, 158.5, 159.0, 159.3; ESI-HRMS for $C_{20}H_{16}N_5O_2S$ (M+H)$^+$ calcd. 390.1025, found 390.1031.

Preparation of *N*-(3-nitrophenyl)isonicotinamide (32)—The general procedure for **8** was followed using 3-nitroaniline (**31**) and isonicotinic acid to afforded **32** (68%) as a yellow solid. ^{1}H NMR (DMSO-d_6, 400 MHz) δ 7.67 – 7.71 (m, 1H), 7.89 – 7.91 (m, 2H), 8.01 (dd, $J_1 = 8.4$ Hz, $J_2 = 1.6$Hz, 1H), 8.19 (dd, $J_1 = 8$ Hz, $J_2 = 1.6$ Hz, 1H), 8.79–8.83 (m, 3H), 10.9 (NH, s, 1H).

Preparation of *N*-(3-aminophenyl)isonicotinamide (33)—*N*-(3-nitrophenyl)isonicotinamide (**32**, 0.823 mmol) in 4 mL ethanol was heated to 70 °C. Then $SnCl_2$•H_2O (4.2 mmol) was added in portions and refluxed until starting material disappeared (~ 4 h). The reaction mixture was cooled and quenched with saturated sodium bicarbonate solution, and extracted with ethyl acetate (3 × 10 mL). The organic layer was washed with saturated sodium bicarbonate, brine, dried over anhydrous sodium sulfate,

filtered and concentrated in vacuo to give a residue, which was used without further purification.

Preparation of (S)-N-(3-(2-(2,3-dichlorophenoxy)propanamido)phenyl)isonicotinamide (34)

The general procedure for **8** was followed using **33** and **7** (R_2 = 2,3-di-ClPh, Y = O, R_3 = (S)-Me) to afford **34** (63%) as a white solid. ^{1}H NMR (CDCl$_3$, 400 MHz) δ 1.67 (d, J = 6.8 Hz, 3H), 4.79 (q, J = 6.8 Hz, 1H), 6.84 – 6.88 (m, 1H), 7.15 – 7.23 (m, 3H), 7.31 (t, J = 8 Hz, 1H), 7.59 (d, J = 8 Hz, 1H), 7.68 (d, J = 4.4 Hz, 2H), 8.02 (s, 1H), 8.24 (s, 1H), 8.68 (s, 1H), 8.75 (s, 2H); ^{13}C NMR (CDCl$_3$, 100 MHz) δ 18.5, 77.0, 111.9, 113.3, 116.5, 117.0, 121.2, 123.0, 124.4, 128.0, 130.0, 134.5, 137.8, 138.3, 142.1, 150.8, 153.7, 164.0, 169.5; ESI-HRMS for $C_{21}H_{18}N_3O_3Cl_2$ (M+H)$^+$ calcd. 430.0725 found 430.0725, Chiral purity (% ee >99, t_R=10.54).

Synthesis of N-(1-phenylethyl)2-pyridin-4-yl)benzo[d]oxazole-5-carboxamide (36)

The general procedure for **8** was followed using **35** and α-methyl benzylamine to give **36** (71%) as a white solid. ^{1}H NMR (CDCl$_3$, 400 MHz) δ 1.57 (d, J = 6.8 Hz, 3H), 5.29 (q, J = 6.8 Hz, 1H), 6.41 (d, J = 7.2 Hz, 1H), 7.19–7.25 (m, 1H), 7.29–7.36 (m, 4H), 7.58 (d, J = 8.4 Hz, 1H), 7.85 (d, J = 8.4 Hz, 1H), 8.00 (d, J = 4.8 Hz, 2H), 8.13 (s, 1H), 8.77 (bs, 2H); ^{13}C NMR (CDCl$_3$, 100 MHz) δ 21.9, 49.7, 111.2, 119.6, 121.3, 126.0, 126.4, 127.8, 129.0, 132.4, 134.0, 142.0, 143.1, 151.0, 152.8, 162.1, 166.1; ESI-HRMS for $C_{21}H_{18}N_3O_2$ (M+H)$^+$ calcd. 344.1399 found 344.1403.

Preparation of 6-nitro-2-(pyridin-4-yl)benzo[d]oxazole (38a)

The general procedure for **3** was followed using 2-amino-5-nitrophenol (**37**) and 4-pyridyl carboxaldehyde to give **38a** (75%) as a yellow solid. ^{1}H NMR (DMSO-d$_6$, 400 MHz) 6.99–7.05 (m, 1H), 8.13 (d, J= 5.2 Hz, 2H), 8.36 (d, J= 8.4 Hz, 1H), 8.89 (d, J = 7.4 Hz, 2H), 8.81 (s, 1H).

Preparation of 2-(pyridin-4-yl)benzo[d]oxazol-6-amine (39a)

The general procedure for **4** was followed using **38a** to obtained **39a** (85%) as a yellow solid. ^{1}H NMR (DMSO-d$_6$, 400 MHz) 5.61 (s, 2H), 6.66 (dd, J_1 = 8 Hz, J_2 = 2 Hz, 1H), 6.79 (d, J = 1.6 Hz, 1H), 7.44 (d, J = 8.8 Hz, 1H), 7.92 (d, J = 6 Hz, 2H), 8.71 (d, J = 6 Hz, 2H).

(S)-2-(2,3-dichlorophenoxy)-N-(2-(pyridin-4-yl)benzo[d]oxazol-6-yl)propionamide (40a)

The general procedure for **8** was followed using **7** (R_2 = 2,3-di-ClPh, Y=O, R_3=(S)-Me) and **39a** to afford **40a** (76%) as a white solid. ^{1}H NMR (CDCl$_3$, 400 MHz) δ 1.71 (d, J = 6.8 Hz, 3H), 4.85 (q, J = 6.6 Hz, 1H), 6.88 (dd, J_1 = 7.2 Hz, J_2 = 2.8 Hz, 1H), 7.12 – 7.18 (m, 2H), 7.24 (dd, J_1 = 8.8 Hz, J_2 = 2 Hz, 2H), 7.69 (d, J = 8.4 Hz, 1H), 7.99 (d, J = 5.6 Hz, 2H), 8.33 (s, 1H), 8.75 (d, J = 5.2 Hz, 2H), 8.91 (s, 1H); ^{13}C NMR (CDCl$_3$, 100 MHz) δ 18.3, 76.7, 102.6, 113.0, 117.4, 120.5, 120.7, 122.6, 124.1, 127.8, 134.0, 134.2, 135.6, 138.3, 150.6, 151.1, 153.4, 160.8, 169.0; ESI-HRMS for $C_{21}H_{16}N_3O_3Cl_2$ (M+H)$^+$ calcd. 428.0569, found 428.0567, Chiral purity (% ee >99, t_R=21.0).

(S)-2-(2,3-dichlorophenoxy)-N-(2-(thiazol-5-yl)benzo[d]oxazol-6-yl)propionamide (40b)

A similar sequence of reactions that was used to prepare **40a** was also used to generate **40b** as a white solid. ^{1}H NMR (CDCl$_3$, 400 MHz) δ 1.73 (d, J = 6.8 Hz, 3H), 4.88 (q, J = 6.4 Hz, 1H), 6.89 – 6.92 (m, 1H), 7.17 – 7.19 (m, 1H), 7.23- 7.26 (m, 2H), 7.66 (d, J = 8.8 Hz, 1H), 8.29 (s, 1H), 8.61 (s, 1H), 8.85 (s, 1H), 8.94(s, 1H); ^{13}C NMR (CDCl$_3$, 100 MHz) δ 18.5, 76.9, 102.8, 113.2, 117.5, 120.1, 122.9, 124.3, 125.7, 128.1, 134.5, 135.4, 138.6, 142.4, 151.0, 153.6, 153.68, 156.2, 157.3, 169.2; ESI-HRMS for

$C_{19}H_{14}N_3O_3SCl_2$ (M+H)$^+$ calcd. 434.0133, found 434.0139, Chiral purity (% ee >99, t_R= 22.5).

Gene cloning, protein expression, purification and crystallization

The coding sequence of *Cp*IMPDH enzyme was amplified by PCR from *Cp*IMPDH-90-134-pET28a plasmid[10b] using primers compatible with the ligation independent cloning vector pMCSG7.[21] The gene was cloned into pMCSG7 using a modified ligation-independent cloning protocol.[22] The recombinant construct produced fusion proteins with an N-terminal His$_6$-tag and a TEV protease recognition site (ENLYFQ↓S). The fusion protein was expressed in an *E. coli* strain BL21(DE3) harboring pMAGIC plasmid encoding one rare *E. coli* Arg tRNAs (covering codons AGG/AGA) in the presence of 100 μg/mL ampicillin and 30 μg/mL kanamycin. The cells were grown in enriched M9 media at 37 °C followed by an overnight induction with 0.5 mM isopropyl-β-D-thiogalactoside (IPTG) at 18 °C. Cells were harvested, resuspended in lysis buffer (50 mM HEPES pH 8.0, 500 mM KCl, 20 mM imidazole, 10 mM 2-mercaptoethanol, 5% glycerol) and stored at –80° C.

*Cp*IMPDH protein was purified according to a standard protocol.[22] The protocol included cell lysis by sonication, Ni^{2+}-affinity chromatography on an ÄKTAxpress system (GE Healthcare Life Sciences) followed by His$_6$-tag cleavage using recombinant TEV protease$_{23}$ and an additional Ni2+-affinity chromatography performed to remove the protease, the uncut protein, and the affinity tag. In the final step, the protein was dialyzed against crystallization buffer containing 20 mM HEPES pH 8.0, 150 mM KCl and 1 mM TCEP, concentrated, flash frozen, and stored in liquid nitrogen. Crystallizations were set up with the help of a Mosquito liquid dispenser (TTP LabTech) using the sitting-drop vapor-diffusion method in 96-well CrystalQuick plates (Greiner Bio-One). For each condition, 0.4 μl protein solution and 0.4 μl crystallization formulation were mixed and equilibrated against a 135 μl reservoir. Five crystallization screens were used. Crystals with IMP and **54** were obtained from a drop solution containing 6 mg/ml protein, 3 mM IMP and 0.5 mM **54**. Diffraction quality crystals appeared at 18 °C in 0.1 M succinic acid pH 7.0 and 15% (w/v) PEG 3350. The crystals were mounted on CryoLoops (Hampton Research) and flash-cooled in liquid nitrogen. The cryoprotectant consisted of 20% ethylene glycol.

Data collection and Structure determination

Diffraction data were collected at 100 K at the 19-ID beamline of the Structural Biology Center at the Advanced Photon Source, Argonne National Laboratory.[24] The single wavelength data at 0.97923 Å (12.661406 keV) up to 2.1 Å were collected from a single crystal of *Cp*IMPDH complexed with IMP and **54**. The crystal was exposed for 5 s per 1.0° rotation of ω with the crystal to detector distance of 300 mm. The data were recorded on a CCD detector Q315 from ADSC scanning 220°. The SBC-Collect program was used for all data collection and visualization. Data collection strategy, integration, and scaling were performed with the HKL3000 program package.[25] A summary of the crystallographic data can be found in Table S1.

The structure was determined by molecular replacement using chain A of the structure of *Cp*IMPDH (PDB ID 3FFS) as a search model with HKL3000 using the data to 3.0 Å.[25] The initial model contained 4 copies of the search model and there was extra electron density for additional protein residues that were not part of the search model. The presence of IMP and **54** in the active site was apparent from the initial electron density map (F_o). Extensive manual model building with coot[26] and the subsequent refinement using phenix.refine[27] was performed against the full data set up to 2.1 Å until the structure converged to the *R* factor (R_{work}) of 0.162, and R_{free} of 0.210 with the r.m.s. bond distances of 0.007 and the r.m.s. bond angles of 1.104°. The asymmetric unit contains four protein chains, A, B, C and D

comprised of residues 1–92 and 135–392 (chains A and C) and 2–92 and 135–392 (chains B and D). The final model also includes four IMP molecules, four **54** molecules, five ethylene glycol molecules and 486 ordered water molecules. Several residues including several N- and C-terminal residues and those introduced as a cloning artifact (SNA)[28] are missing due to disorder. In addition, residues 312–325 of chain A, 309–235 of chain B, 311–325 of chains C and D located on the surface of the tetramer were disordered and not modeled. The stereochemistry of the structure was checked with PROCHECK[29] and the Ramachandran plot. Atomic coordinates and experimental structure factors of the structure have been deposited in the PDB under the ID code 4IXH.

Inhibition of recombinant *Cp*IMPDH

Recombinant *Cp*IMPDH, purified from *E. coli*,[12] was assessed by monitoring the production of NADH by fluorescence at varying inhibitor concentrations (25 pM – 5 YM). IMPDH was incubated with inhibitor for 5 min at room temperature prior to addition of substrates. The following conditions were used: 50 mM Tris-HCl, pH 8.0, 100 mM KCl, 3 mM EDTA, 1 mM dithiothreitol (assay buffer) at 25 °C, 10 nM *Cp*IMPDH, 300 μM NAD and 150 μM IMP. To characterize the non-specific binding of inhibitors, assays were also carried out in the presence of 0.05% BSA (fatty acid free). IC_{50} values were calculated for each inhibitor according to Equation 1 using the SigmaPlot program (SPSS, Inc.):

$$\upsilon_i = \upsilon_o/(1+[I]/IC_{50}) \quad \text{(Eq. 1)}$$

where υ_i is initial velocity in the presence of inhibitor (I) and υ_o is the initial velocity in the absence of inhibitor. When the values of IC_{50} approach the concentration of enzyme, tight binding treatment is used:

$$\upsilon_i/\upsilon_o = 1 - (([E]+[I]+IC_{50}) - (([E]+[I]+IC_{50})^2 - 4[E][I])^{0.5})/2[E] \quad \text{(Eq. 2)}$$

Inhibition at each inhibitor concentration was measured in quadruplicate and averaged; this value was used as υ_i. The IC_{50} values were determined three times; the average and standard deviations are reported. Mechanism of inhibition was determined by fitting to equations for competitive, noncompetitive/mixed and uncompetitive inhibition as previously described.[16c]

Supplementary Material

Refer to Web version on PubMed Central for supplementary material.

Acknowledgments

Abbreviations

Cp	*Cryptosporidium parvum*
CL_{int}	intrinsic clearance
BSA	bovine serum albumin

DCM	dichloromethane
DEAD	Diethylazodicarboxylate
DIPEA	diisopropylethylamine
DMF	*N*,*N*-dimethylformamide
EDCI•HCl	1-Ethyl-3-(3-dimethylaminopropyl)carbodiimide hydrochloride
IMP	inosine 5′-monophosphate
IMPDH	inosine 5′-monophosphate dehydrogenase
hIMPDH	human IMPDH
HTS	high-throughput screening
MPA	mycophenolic acid
MR	molecular replacement
N.D	not determined
r.m.s	root-mean-square
TEA	triethylamine
Toxo	*Toxoplasma*
XMP	xanthosine 5′-monophosphate

References

1. (a) Carey CM, Lee H, Trevors JT. Biology, persistence and detection of *Cryptosporidium parvum* and *Cryptosporidium hominis* oocyst. Water Res. 2004; 38:818–62. [PubMed: 14769405] (b) Fayer R. Cryptosporidium: a water-borne zoonotic parasite. Veterinary Parasitology Veterinary parasitology. 2004; 126:37–56.

2. Guerrant RL, Oriá RB, Moore SR, Oriá MOB, Lima AAM. Malnutrition as an enteric infectious disease with long-term effects on child development. Nutrition Reviews. 2008; 66:487–505. [PubMed: 18752473]

3. Snelling WJ, Xiao L, Ortega-Pierres G, Lowery CJ, Moore JE, Rao JR, Smyth S, Millar BC, Rooney PJ, Matsuda M, Kenny F, Xu J, Dooley JSG. Cryptosporidiosis in developing countries. 2007; 1

4. DuPont HL, Chappell CL, Sterling CR, Okhuysen PC, Rose JB, Jakubowski W. The infectivity of *Cryptosporidium parvum* in healthy volunteers. N Engl J Med. 1995; 332:855–859. [PubMed: 7870140]

5. Mead JR. Cryptosporidiosis and the challenges of chemotherapy. Drug resistance updates: reviews and commentaries in antimicrobial and anticancer chemotherapy. 2002; 5:47–57. [PubMed: 12127863]

6. (a) Striepen B, Pruijssers AJ, Huang J, Li C, Gubbels MJ, Umejiego NN, Hedstrom L, Kissinger JC. Gene transfer in the evolution of parasite nucleotide biosynthesis. Proc Natl Acad Sci USA. 2004; 101:3154–3159. [PubMed: 14973196] (b) Xu P, Widmer G, Wang Y, Ozaki LS, Alves JM, Serrano MG, Puiu D, Manque P, Akiyoshi D, Mackey AJ, Pearson WR, Dear PH, Bankier AT, Peterson DL, Abrahamsen MS, Kapur V, Tzipori S, Buck GA. The genome of Cryptosporidium hominis. Nature. 2004; 431:1107–1112. [PubMed: 15510150] (c) Abrahamsen MS, Templeton TJ, Enomoto S, Abrahante JE, Zhu G, Lancto CA, Deng M, Liu C, Widmer G, Tzipori S, Buck GA, Xu P, Bankier AT, Dear PH, Konfortov BA, Spriggs HF, Iyer L, Anantharaman V, Aravind L, Kapur V. Complete genome sequence of the apicomplexan, Cryptosporidium parvum. Science. 2004; 304:441–445. [PubMed: 15044751]

7. Hedstrom L. IMP Dehydrogenase: structure, mechanism and inhibition. Chem Rev. 2009; 109:2903 – 2928. [PubMed: 19480389]

8. Striepen B, White MW, Li C, Guerini MN, Malik SB, Logsdon JM Jr, Liu C, Abrahamsen MS. Genetic complementation in apicomplexan parasites. Proc Natl Acad Sci USA. 2002; 99:6304– 6309. [PubMed: 11959921]

9. Umejiego NN, Gollapalli D, Sharling L, Volftsun A, Lu J, Benjamin NN, Stroupe AH, Riera TV, Striepen B, Hedstrom L. Targeting a prokaryotic protein in a eukaryotic pathogen: identification of lead compounds against cryptosporidiosis. Chem Biol. 2008; 15:70–77. [PubMed: 18215774]

10. (a) Maurya SK, Gollapalli DR, Kirubakaran S, Zhang M, Johnson CR, Benjamin NN, Hedstrom L, Cuny GD. Triazole inhibitors of *Cryptosporidium parvum* inosine 5′-monophosphate dehydrogenase. J Med Chem. 2009; 52:4623–4630. [PubMed: 19624136] (b) MacPherson IS, Kirubakaran S, Gorla SK, Riera TV, D'Aquino JA, Zhang M, Cuny GD, Hedstrom L. The structural basis of Cryptosporidium-specific IMP dehydrogenase inhibitor selectivity. J Am Chem Soc. 2010; 132:1230–1231. [PubMed: 20052976] (c) Gorla, SK.; Johnson, C.; Khan, J.; Sun, X.; Sharling, L.; Striepen, B.; Hedstrom, L. Targeting Prokaryotic Enzymes in the Eukaryotic Pathogen Cryptosporidium. In: Becker, K., editor. Apicomplexan Parasites. Vol. 2. Wiley-VCH Verlag GmbH & Co. KGaA; Weinheim, Germany: 2011. Chapter 14(d) Kirubakaran S, Gorla SK, Sharling L, Zhang M, Liu X, Ray SS, MacPherson IS, Striepen B, Hedstrom L, Cuny GD. Structure–activity relationship study of selective benzimidazole-based inhibitors of Cryptosporidium parvum IMPDH. Bioorg Med Chem Lett. 2012; 22:1985–1988. [PubMed: 22310229] (e) Gorla SK, Kavitha M, Zhang M, Liu X, Sharling L, Gollapalli DR, Striepen B, Hedstrom L, Cuny GD. Selective and potent urea inhibitors of Cryptosporidium parvum inosine monophosphate dehydrogenase. J Med Chem. 2012; 55:7759–7771. [PubMed: 22950983] (f) Johnson CR, Gorla SK, Kavitha M, Zhang M, Liu X, Striepen B, Mead JR, Cuny GD, Hedstrom L. Phthalazinone inhibitors of inosine-5′-monophosphate dehydrogenase from Cryptosporidium parvum. Bioorg Med Chem Lett. 2013; 23:1004–1007. [PubMed: 23324406]

11. Kawashita Y, Nakamichi N, Kawabata H, Hayashi M. Direct and practical synthesis of 2-arylbenzoxazoles promoted by activated carbon. Org Lett. 2003; 5:3713–3715. [PubMed: 14507212]

12. Bui, M.; Conlon, P.; Erlanson, DA.; Fan, J.; Guan, B.; Hopkins, BT.; Ishchenko, A.; Jenkins, TJ.; Kumaravel, G.; Marcotte, D.; Powell, N.; Scott, D.; Taveras, A.; Wang, D.; Zhong, M. Preparation of 4-(3-aminopiperidin-1-yl)-7H-pyrrolo[2,3-d]pyrimidine and 4-(3-aminopiperidin-1-yl)pyrimidine derivatives as Bruton's tyrosine kinase (Btk kinase) inhibitors. WO 2011029043. 2011.

13. Petit M, Lapierre AJB, Curran DP. Relaying asymmetry of transient atropisomers of o-iodoanilides by radical cyclizations. J Am Chem Soc. 2005; 127:14994–14995. [PubMed: 16248616]

14. Mori K. Synthesis of (*R*)-*ar*-turmerone and its conversion to (*R*)-*ar*-himachalene, a pheromone component of the flea beetle: (*R*)-*ar*-himachalene is dextrorotatory in hexane, while levorotatory in chloroform. Tetrahedron: Asymmetry. 2005; 16:685–692.

15. (a) Sharpless KB, Manetsch R. In situ click chemistry: a powerful means for lead discovery. Exp Opin Drug Discovery. 2006; 1:525–538.(b) Kolb HC, Sharpless KB. The growing impact of click chemistry on drug discovery. Drug Discovery Today. 2003; 8:1128–1137. [PubMed: 14678739] (c) Finn MG, Sharpless KB. Click chemistry: diverse chemical function from a few good reactions. Angew Chem, Int Ed. 2001; 40:2004–2021.

16. (a) Farazi T, Leichman J, Harris T, Cahoon M, Hedstrom L. Isolation and characterization of mycophenolic acid resistant mutants of inosine 5′monophosphate dehydrogenase. J Biol Chem. 1997; 272:961–965. [PubMed: 8995388] (b) Mortimer SE, Hedstrom L. Autosomal dominant retinitis pigmentosa mutations in inosine 5′-monophosphate dehydrogenase type I disrupt nucleic acid binding. Biochem J. 2005; 390(Pt 1):41–47. [PubMed: 15882147] (c) Umejiego NN, Li C, Riera T, Hedstrom L, Striepen B. Cryptosporidium parvum IMP dehydrogenase: Identification of functional, structural and dynamic properties that can be exploited for drug design. J Biol Chem. 2004; 279:40320–40327. [PubMed: 15269207]

17. (a) Merrikin DJ, Briant J, Rolinson GN. Effect of protein binding on antibiotic activity in vivo. J Antimicrob Chemother. 1983; 11:233–238. [PubMed: 6841305] (b) Craig WA, Ebert SC. Protein binding and its significance in antibacterial therapy. Infect Dis Clin North Am. 1989; 3:407–414. [PubMed: 2671130] (c) Smith DA, Di L, Kerns EH. The effect of plasma protein binding on in

vivo efficacy: misconceptions in drug discovery. Nat Rev Drug Discov. 2010; 9:929–939. [PubMed: 21119731]

18. Sharling L, Liu X, Gollapalli DR, Maurya SK, Hedstrom L, Striepen B. A screening pipeline for antiparasitic agents targeting *Cryptosporidium* inosine monophosphate dehydrogenase. PLoS Negl Trop Dis. 2010; 4:e794. [PubMed: 20706578]

19. Sintchak MD, Fleming MA, Futer O, Raybuck SA, Chambers SP, Caron PR, Murcko MA, Wilson KP. Structure and mechanism of inosine monophosphate dehydrogenase in complex with the immunosuppressant mycophenolic acid. Cell. 1996; 85:921 – 930. [PubMed: 8681386]

20. Gubbels MJ, Striepen B. Studying the cell biology of apicomplexan parasites using fluorescent proteins. Microsc Microanal. 2004; 10:568–579. [PubMed: 15525431]

21. Stols L, Gu M, Dieckman L, Raffen R, Collart FR, Donnelly MI. A new vector for high-throughput, ligation-independent cloning encoding a tobacco etch virus protease cleavage site. Protein Expr Purif. 2002; 25:8–15. [PubMed: 12071693]

22. Kim Y, Babnigg G, Jedrzejczak R, Eschenfeldt WH, Li H, Maltseva N, Hatzos-Skintges C, Gu M, Makowska-Grzyska M, Wu R, An H, Chhor G, Joachimiak A. High-throughput protein purification and quality assessment for crystallization. Methods. 2011; 55:2–28.

23. Blommel PG, Fox BG. A combined approach to improving large-scale production of tobacco etch virus protease. Protein Expr Purif. 2007; 55:53–68. [PubMed: 17543538]

24. Rosenbaum G, Alkire RW, Evans G, Rotella FJ, Lazarski K, Zhang RG, Ginell SL, Duke N, Naday I, Lazarz J, Molitsky MJ, Keefe L, Gonczy J, Rock L, Sanishvili R, Walsh MA, Westbrook E, Joachimiak A. The Structural Biology Center 19ID undulator beamline: Facility specifications and protein crystallographic results. J Synchrotron Radiat. 2006; 13(Pt 1):30–45. [PubMed: 16371706]

25. Minor W, Cymborowski M, Otwinowski Z, Chruszcz M. HKL-3000: The integration of data reduction and structure solution--from diffraction images to an initial model in minutes. Acta Crystallogr D Biol Crystallogr. 2006; 62:859–866. [PubMed: 16855301]

26. Emsley P, Cowtan K. Coot: Model-building tools for molecular graphics. Acta Crystallogr Section D. 2004; 60:2126–2132. [PubMed: 15572765]

27. Adams PD, Afonine PV, Bunkóczi G, Chen VB, Davis IW, Echols N, Headd JJ, Hung LW, Kapral GJ, Grosse-Kunstleve RW, McCoy AJ, Moriarty NW, Oeffner R, Read RJ, Richardson DC, Richardson JS, Terwilliger TC, Zwart PH. PHENIX: A comprehensive Python-based system for macromolecular structure solution. Acta Crystallogr D Biol Crystallogr. 2010; 66:213–221. [PubMed: 20124702]

28. Kim Y, Dementieva I, Zhou M, Wu R, Lezondra L, Quartey P, Joachimiak G, Korolev O, Li H, Joachimiak A. Automation of protein purification for structural genomics. J Struct Funct Genomics. 2004; 5:111–118. [PubMed: 15263850]

29. Laskowski RA, MacArthur MW, Moss DS, Thornton JM. PROCHECK: A program to check the stereochemical quality of protein structures. J Appl Cryst. 1993; 26:283–291.
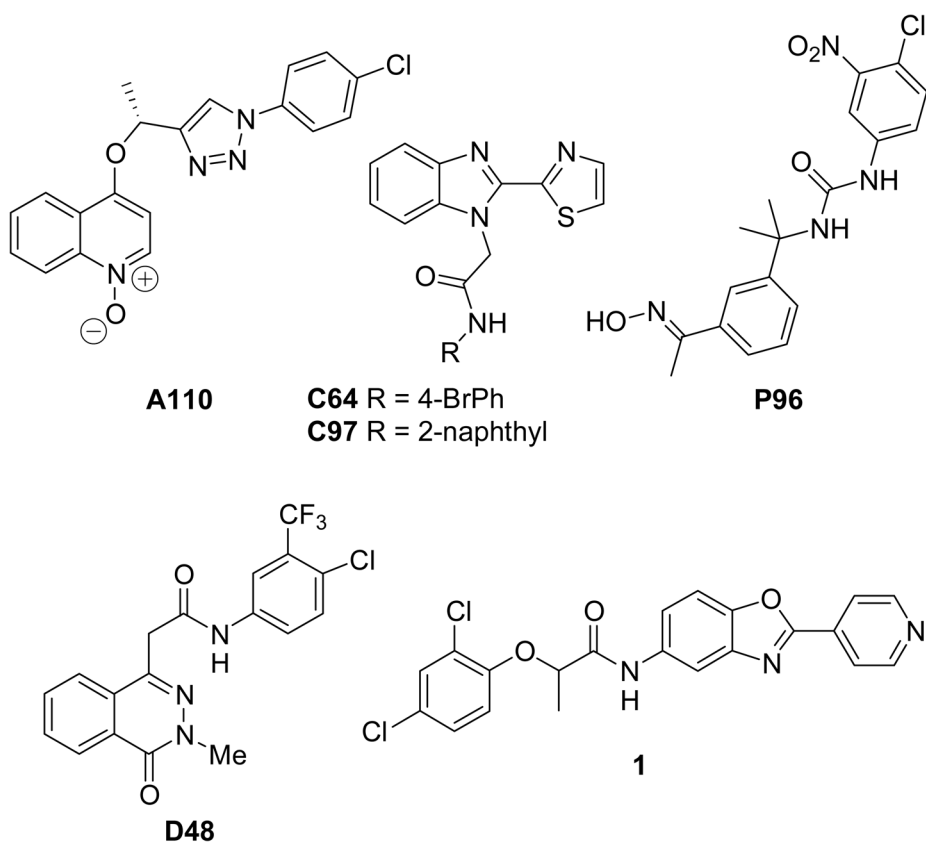
Figure 1.
Optimized *Cp*IMPDH inhibitors **A110**, **C64**, **C97**, **P96** and **D48** and *Cp*IMPDH inhibitor **1** identified by HTS.
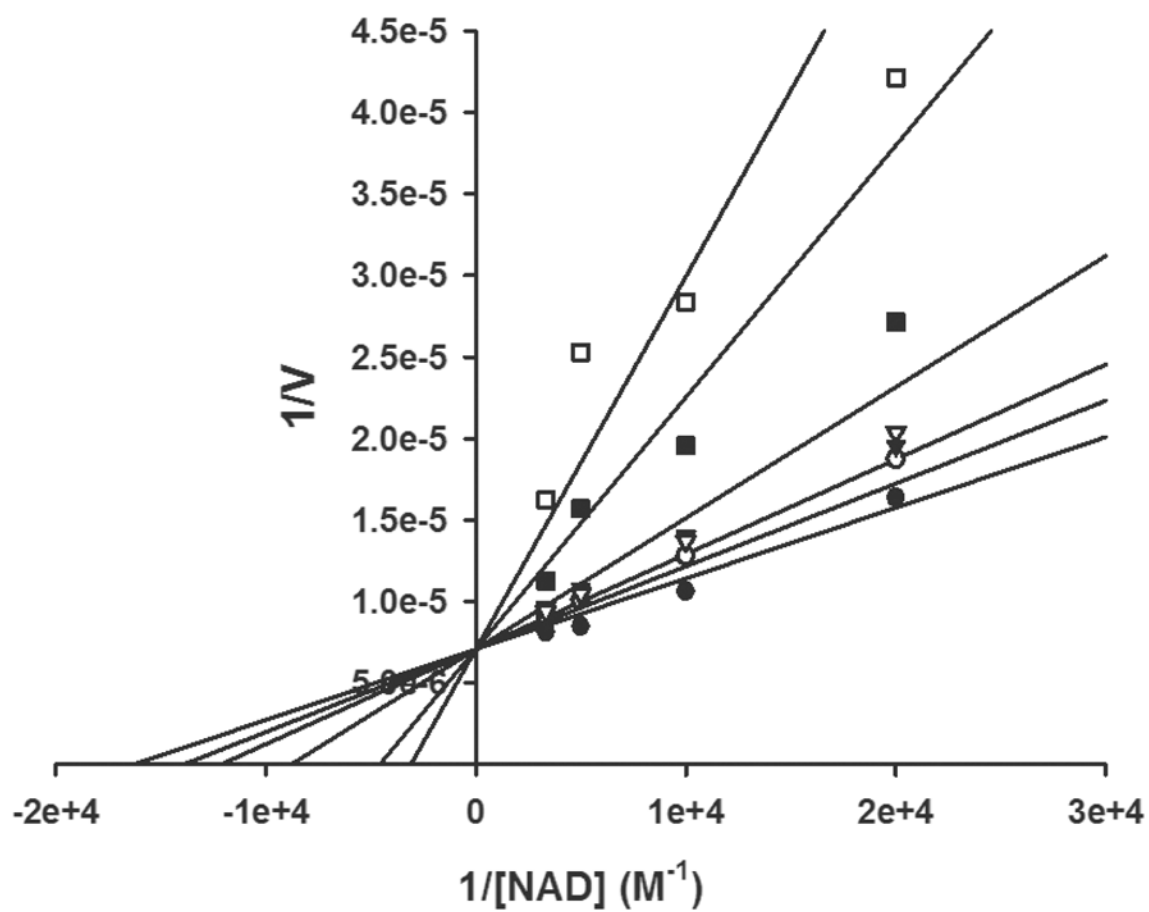
Figure 2.
Inhibition of *Cp*IMPDH by **68**. Inhibitor concentrations: open squares, 630 nM; closed squares, 380 nM; closed triangles, 130 nM; open triangles, 50 nM; open circles, 25 nM; no inhibitor, closed circles.
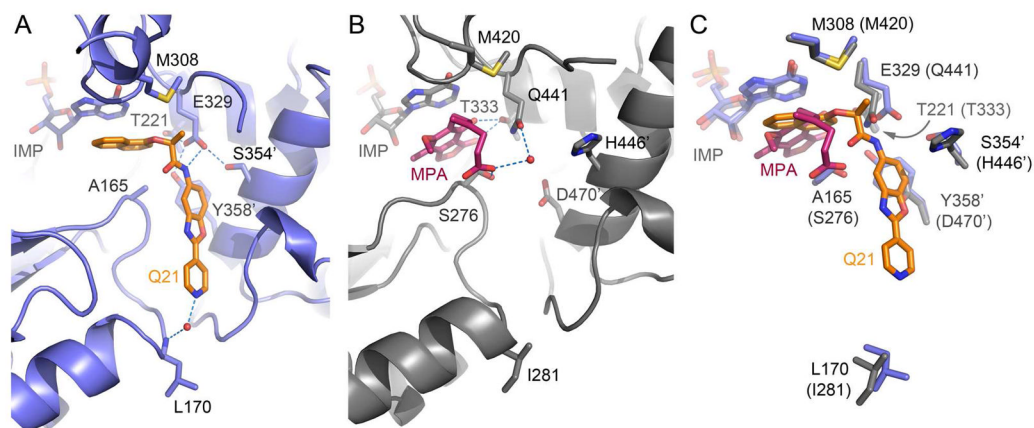
Figure 3.
The inhibitor binding site in IMPDH. (**A**) Structure of *Cp*IMPDH in complex with IMP and **54** (violet-blue; PDB ID code 4IXH). (**B**) Structure of Chinese hamster IMPDH (gray; PDB ID code)[19] in complex with IMP and MPA. (**C**) Overlay of *C. parvum* and Chinese hamster active sites. IMP, **54**, MPA and residues interacting with the inhibitors are shown as sticks. Numbers in parentheses in panel C indicate Chinese hamster labeling. Water molecules are shown as red spheres and hydrogen bonding interactions are shown as blue dashed lines. An apostrophe indicates a residue from the adjacent monomer.
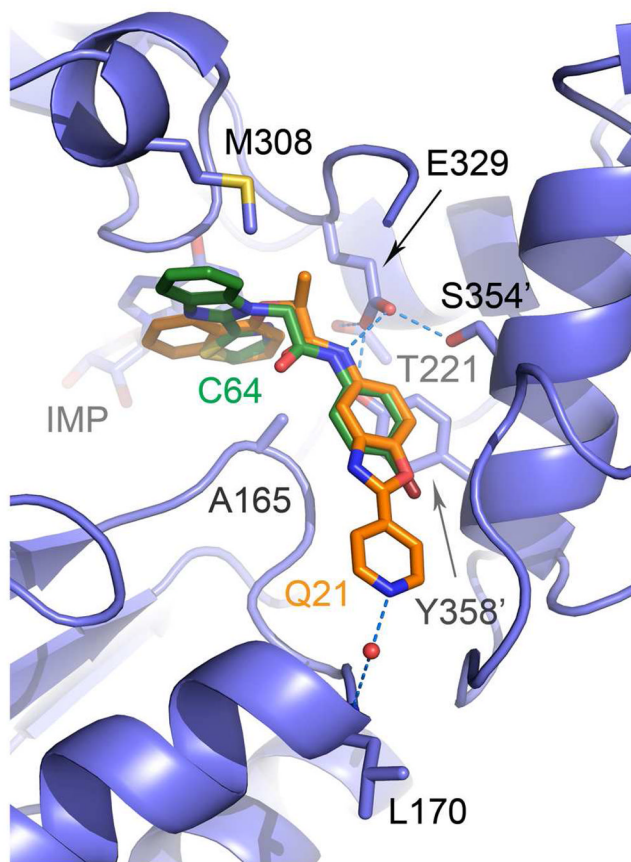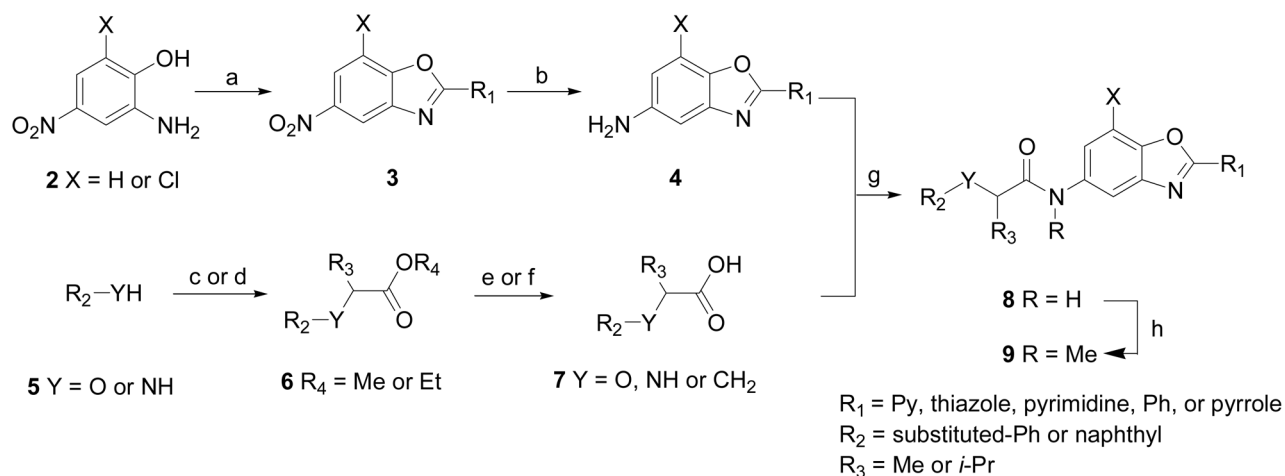
Figure 4.
Overlay of *Cp*IMPDH structures with **54** (violet-blue; PDB ID code 4IXH) and **C64** (PDB ID code 3KHJ).[10b] IMP, **54**, **C64** and the interaction residues are shown as sticks. A water molecule is shown as a red sphere and hydrogen bonding interactions are shown as blue dashed lines. An apostrophe denotes a residue from the adjacent monomer.
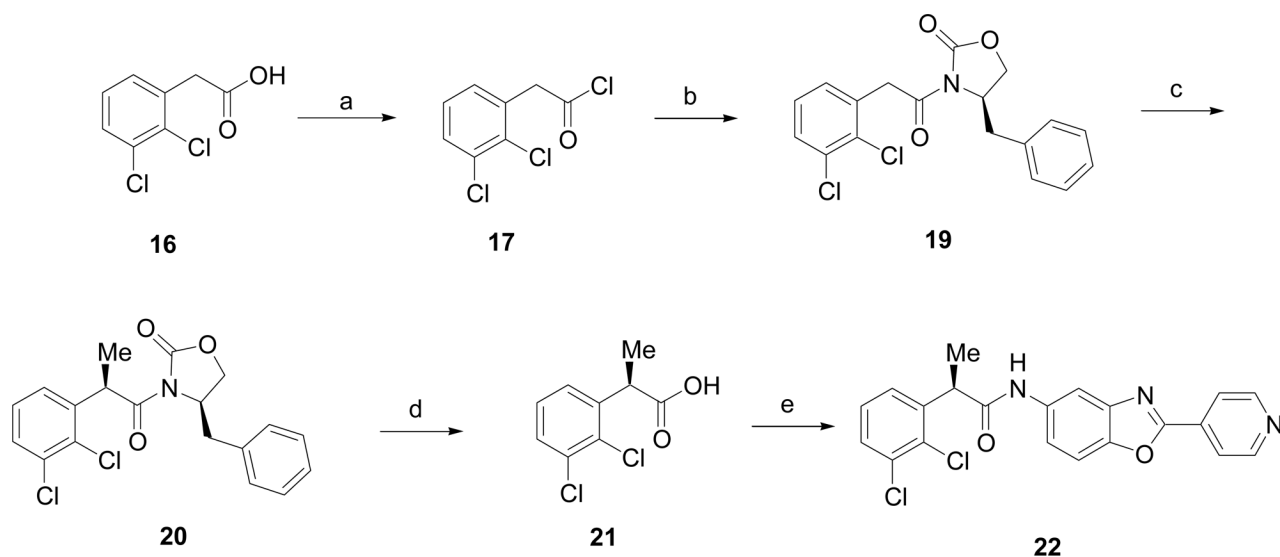
Scheme 1.

General procedure for the synthesis of benzoxazole derivatives.

Reagents and conditions: (a) R_1-CHO, O_2, DarcoKB, xylene, 120 °C, 6 h, 70–80% (b) H_2 (1 atm), 10% Pd-C, EtOAc, 6 h, 80–86% (c) R_3CHBrCOOR_4, K_2CO_3, DMF, rt, 5 h, 85–92% when Y = O (or 70 °C, 3 h, 36% when Y = NH) (d) (*R*)- or (*S*)- R_3CH(OH)COOR_4, 0 °C, PPh$_3$, 10 min, DEAD, rt, 12 h, 75–84% (e) 3 M NaOH, THF:H$_2$O (2:1), 80 °C, 3 h, 85–95% (f) 3N HCl, THF, 70 °C, 6 h, 60–70% (g) EDCI•HCl, DMF, 0 °C - rt, 12 h, 63–79% (h) MeI, NaH, THF, 0 °C - rt, 1.5 h, 48%.
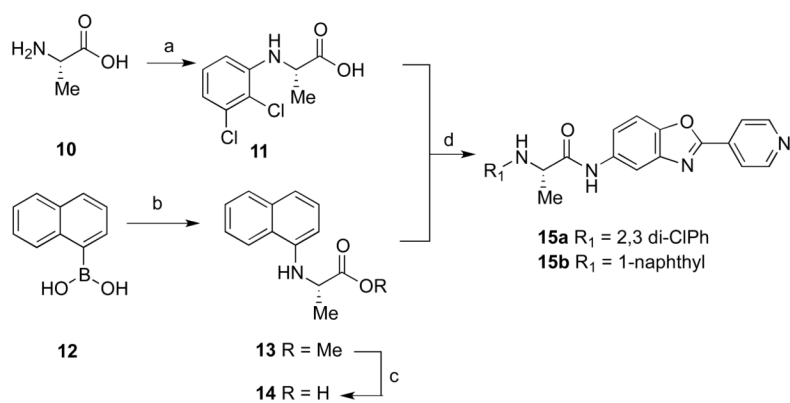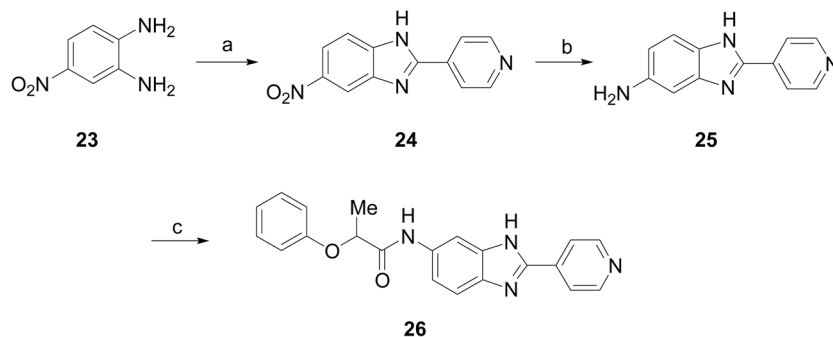
Scheme 2.

General procedure for the synthesis of enantiomerically pure secondary amines of 5-benzoxazoles.

Reagents and conditions: (a) 2,3-di-ClPhI, Cs_2CO_3, CuI, DMF, 90 °C, 48 h, 57% (b) L-alanine methyl ester hydrochloride, $Cu(OAc)_2$, DCM, TEA, oxygen, 4Å molecular sieves, rt, 48 h, 34% (c) 1 M NaOH, MeOH, rt, 12 h, 67% (d) **4**, EDCI•HCl, DMF, 0 °C - rt, 12 h, 60–70%.

Scheme 3.

Synthesis of a 2-phenylpropionamide benzoxazole derivative.

Reagents and conditions: (a) $SOCl_2$, 90 °C, 2 h (b) **18**, *n*-BuLi (2.5 M), THF, −78 °C to 0 °C, 1 h, 80% (c) (i) NaN(TMS)$_2$ in THF, −78 °C, 1 h (ii) MeI, THF, −78 °C, 2 h (iii) rt, 5 h, 77% (d) Li_2O_2, THF, H_2O, 0 °C, 1 h, 87% (e) **4** (R$_1$ = 4-Py, X = H), EDCl•HCl, DMF, 0 °C - rt, 12 h, 70%.
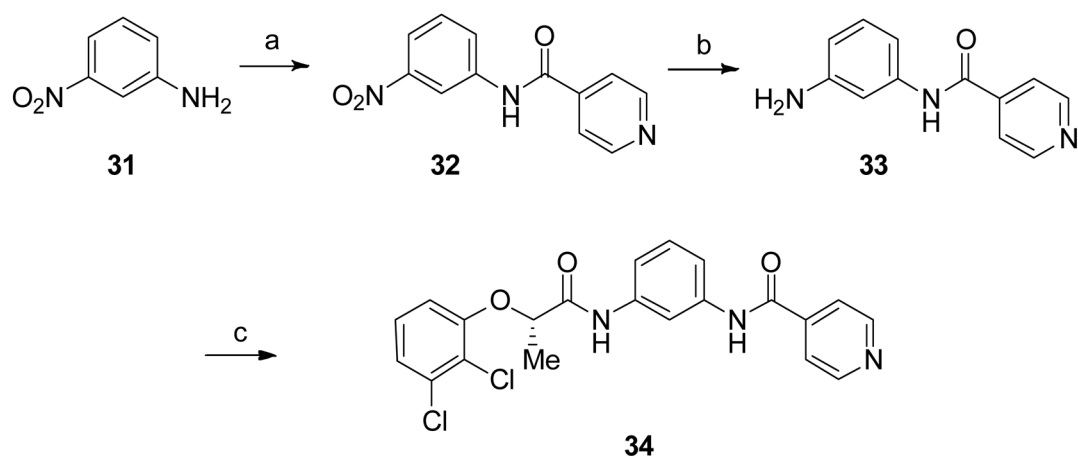
Scheme 4.

Synthesis of a benzimidazole derivative.

Reagents and conditions: (a) 4-PyCHO, $Na_2S_2O_5$, DMF, 120 °C, 24 h, 61% (b) H_2 (1 atm), 10% Pd-C, MeOH, rt, 6 h, 64% (c) PhOCH(CH$_3$)COCl, TEA, cat. 4-DMAP, THF, 0 °C – rt, 30 min, 70%. A benzimidazole analogue of **1** was prepared using the method outlined in Scheme 4. 6-Nitro-2-(pyridin-4-yl)-1*H*-benzo[*d*]imidazole (**24**) was prepared by condensation of 4-pyridine carboxaldehyde with 4-nitro-1,2-phenylenediamine (**23**) in the presence of the oxidizing agent sodium metabisulphite.[10d] The product was reduced in the presence of hydrogen (1 atm) and 10% Pd-C to give **25**, which was then coupled with 2-(phenoxy)propionyl chloride in the presence of triethylamine and catalytic DMAP to give **26**.
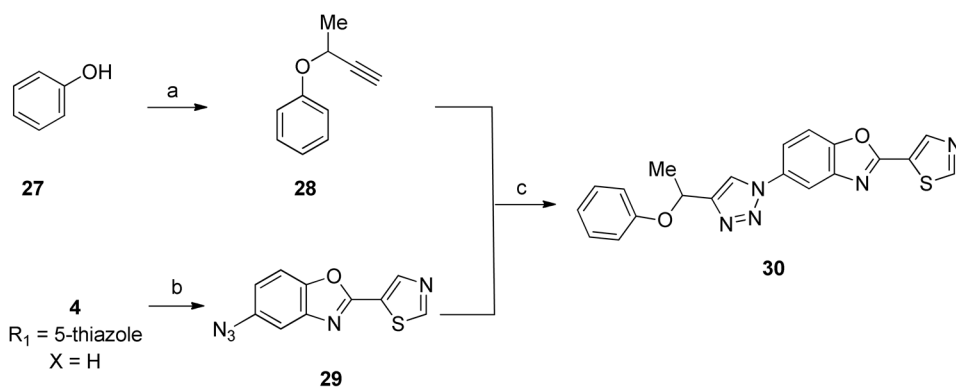
Scheme 5.
Synthesis of a 1,2,3-triazole derivative.
Reagents and conditions: (a) $CH_3CH(OH)C \equiv CH$, PPh_3, 0 °C, 10 min then DEAD, THF, 70 °C, 20 h, 69% (b) $NaNO_2$, HCl, H_2O, NaN_3, -5 °C – 0 °C, 1.5 h, 89% (c) CH_3CN, DIPEA, CuI, rt, 50 min, 84%.

Scheme 6.
Synthesis of an 1,3-diamide derivative.
Reagents and conditions: (a) 4-PyCO$_2$H, EDCI•HCl, DCM, 0 °C - rt, 12 h, 68% (b)
SnCl$_2$•H$_2$O, EtOH, 70 °C, 4 h, 62% (c) (*S*)- 2,3-di-Cl-PhOCH(CH$_3$)COOH, EDCI•HCl,
DCM, 0 °C - rt, 12 h, 63%.
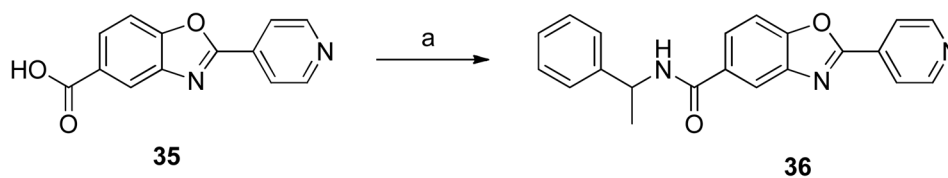
Scheme 7.
Synthesis of amide derivative **36**.
Reagents and conditions: (a) α-methyl benzyl amine, EDCI•HCl, DMF, 0 °C - rt, 12 h, 71%.
An analogue of **22** in which the amide group is inverted was prepared using the method outlined in Scheme 7. Amide **36** was generated by coupling 2-(pyridin-4-yl)benzo[d]oxazole-5-carboxylic acid (**35**) and α-methylbenzylamine in the presence of EDCI•HCl.
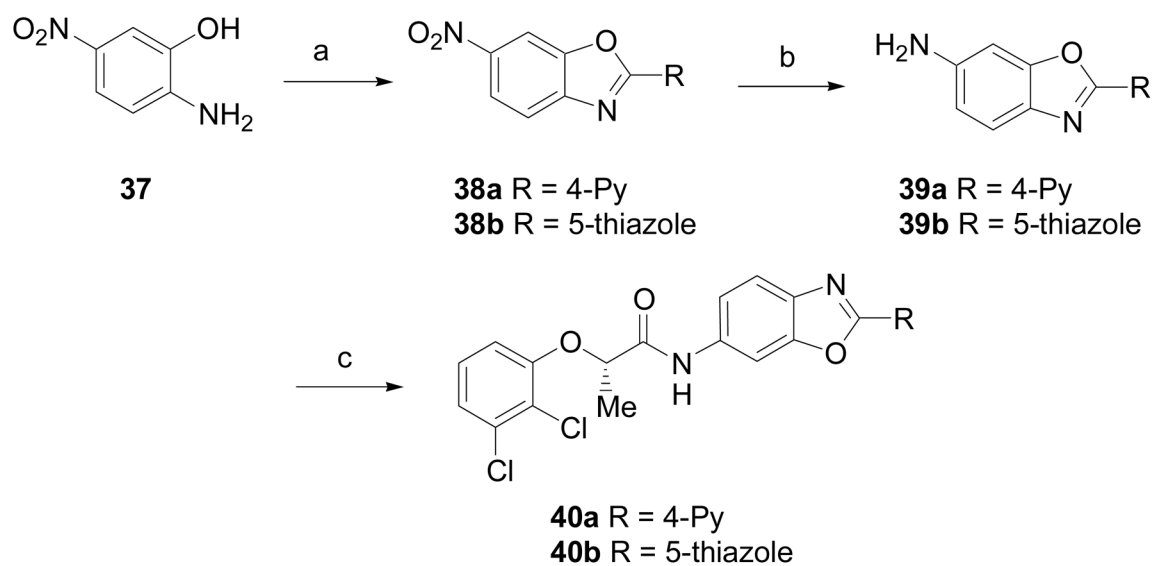
Scheme 8.
General procedure for the synthesis of 6-substituted benzoxazole derivatives.
Reagents and conditions: (a) RCHO, O_2, DarcoKB, xylene, 120 °C, 6 h, 75% (b) H_2 (1 atm), 10% Pd-C, EtOAc, rt, 6 h, 85% (c) (*S*)-2,3-di-Cl-PhOCH(CH$_3$)COOH, EDCI•HCl, DMF, 0 °C - rt, 12 h, 76%.

Table 1

SAR of phenyl ring of **1** for *Cp*IMPDH inhibition.
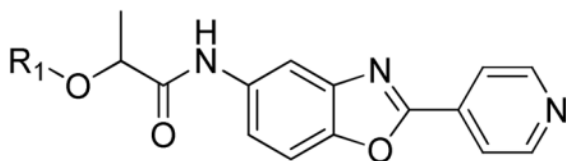
ID	R$_1$	IC$_{50}$ (nM)	
		(−) BSA	(+) BSA
1	2,4-di-ClPh	44 ± 8	120 ± 10
41	2-ClPh	19 ± 2	50 ± 10
42	4-ClPh	105 ± 17	118 ± 3
43	Ph	40 ± 5	50 ± 20
44	4-OMePh	28 ± 2	34 ± 5
45	3-ClPh	20 ± 7	32 ± 8
46	2,3-di-ClPh	3 ± 1	11 ± 1
47	2,6-di-ClPh	>5000 [*]	n.d
48	1-naphthyl	9 ± 3	14 ± 6
49	1-(4-Cl-naphthyl)	27 ± 1	53 ± 9

[*] One determination, n.d. = not determined.

Table 2

SAR of amide α-position of **1** for *Cp*IMPDH inhibition.
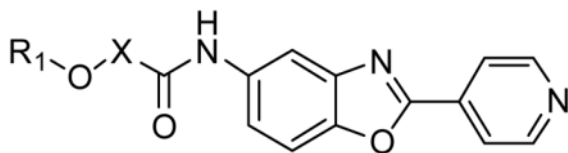
ID	X	R$_1$	IC$_{50}$ (nM)	
			(−) BSA	(+) BSA
50	CH$_2$	2,4-di-ClPh	>5000*	n.d
51	CMe$_2$	4-ClPh	>5000*	n.d
52	CH-i-Pr	1-naphthyl	24 ± 2	57 ± 5
53	(R)-CHMe	1-naphthyl	400 ± 70	380 ± 60
54	(S)-CHMe	1-naphthyl	6.1 ± 0.5	8 ± 3
55	(S)-CHMe	2,3-di-ClPh	1.2 ± 0.2	3.5 ± 0.7
56	(S)-CHMe	2-Cl,3-CF$_3$Ph	9 ± 1	52 ± 5
57	(S)-CHMe	2-Cl,3-NO$_2$Ph	2.3 ± 0.9	6 ± 4
58	(S)-CHMe	2,3-di-OMePh	50 ± 10	60 ± 20

*One determination, n.d. = not determined.

Table 3

SAR of the pyridine ring of **1** for *Cpl*MPDH inhibition.
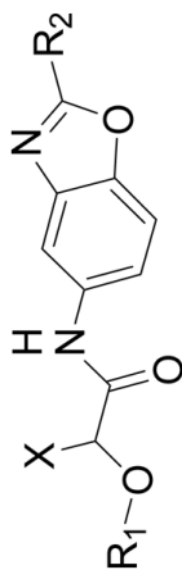
ID	X	R₁	R₂	IC₅₀ (nM)	
				(−) **BSA**	(+) **BSA**
59	Me	2,4-di-ClPh	Ph	>5000*	n.d
60	Me	2,4-di-ClPh	3-Py	150 ± 20	600 ± 200
61	Me	2,4-di-ClPh	2-Py	210 ± 20	800 ± 200
62	(*S*)-Me	2,3-di-ClPh		1.4 ± 0.3	2.3 ± 0.4
63	(*S*)-Me	1-naphthyl		2.7 ± 0.7	4.0 ± 0.9
64	Me	1-(4-Cl-naphthyl)		28 ± 6	70 ± 10
65	(*S*)-Me	2,3-di-ClPh		17 ± 6	30 ± 10
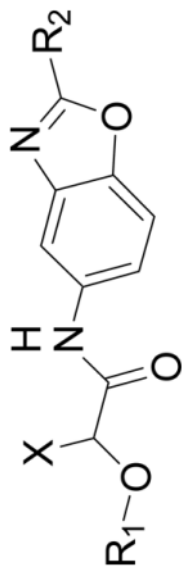
ID	X	R₁	R₂	IC₅₀ (nM) (−) BSA	IC₅₀ (nM) (+) BSA
66	(*S*)-Me	1-naphthyl		26 ± 5	50 ± 5
67	Me	1-naphthyl		$>5000^*$	n.d

*One determination, n.d. = not determined.

Table 4

Other miscellaneous changes to explore the SAR of **1** for *Cp*IMPDH inhibition.

ID	Structure	IC$_{50}$ (nM)	
		(−) BSA	(+) BSA
30		>5000[*]	n.d.
9		>5000[*]	n.d.
36		>5000[*]	n.d.
40a		0.6 ± 0.5	4 ± 2
40b		7 ± 1	60 ± 20
68		240 ± 90	600 ± 300
26		>5000[*]	n.d.
34		>5000[*]	n.d.

[*] One determination, n.d. = not determined.

Table 5

SAR of benzyl amide derivatives of **1** for *Cp*IMPDH inhibition.
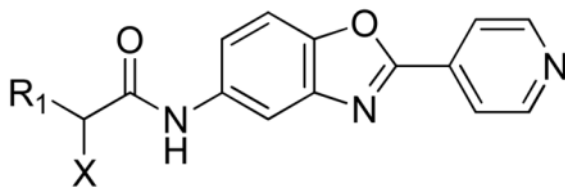
ID	X	R$_1$	IC$_{50}$ (nM)	
			(-) BSA	(+) BSA
69	Me	CH$_2$Ph	> 5000	n.d.
70	Me	Ph	120 ± 20	130 ± 30
71	(*S*)-Me	Ph	>5000*	n.d.
72	(*R*)-Me	Ph	22.3 ± 5.9	28.0 ± 3.5
22	(*R*)-Me	2,3-di-ClPh		60 ± 3

Table 6

SAR of secondary amine derivatives of **1** for *Cp*IMPDH inhibition.
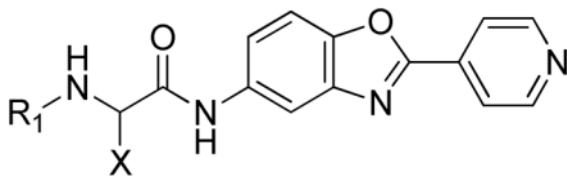
ID	X	R$_1$	IC$_{50}$ (nM)	
			(−) BSA	(+) BSA
73	Me	2,3-di-ClPh	2 ± 1	1.8 ± 0.5
15a	(*S*)- Me	2,3-di-ClPh	0.5 ± 0.1	1.1 ± 0.1
15b	(*S*)- Me	1-naphthyl	14 ± 6	15 ± 3

Table 7

Mechanism of inhibition of CpIMPDH by selected compounds.

Cmpd	Substrate	Mechanism	K_{is} (nM)
1	IMP	NC	58 ± 5
	NAD	C	33 ± 8
63[a]	IMP	NC	1.6 ± 0.7
	NAD	C	0.9 ± 0.3
68	IMP	NC	210 ± 10
	NAD	C	150 ± 30
72	IMP	NC	100 ± 20
	NAD	C	40 ± 10

[a]Q26 was analyzed using tight binding treatment;

NC: noncompetitive; C: competitive.

NIH-PA Author Manuscript

NIH-PA Author Manuscript

NIH-PA Author Manuscript

Table 8

NADPH-dependent mouse liver microsomal stability.

ID	Connection	R₁	R₂	X	Y	t₁/₂ (min)	
						+ NADPH	− NADPH
54	5	1-naphthyl	4-Py	(S)-Me	O	30	--
55	5	2,3-di-ClPh	4-Py	(S)-Me	O	9.0	12
62	5	2,3-di-ClPh	5-thiazolyl	(S)-Me	O	7.0	11
72	5	Ph	4-Py	(R)-Me	---	43	130[a]
22	5	2,3-di-ClPh	4-Py	(R)-Me	---	25	130
15a	5	2,3-di-ClPh	4-Py	(S)-Me	NH	44	110
15b	5	1-naphthyl	4-Py	(S)-Me	NH	18	27
40a	6	2,3-di-ClPh	4-Py	(S)-Me	NH	10	9

[a]Estimated from a single time point at 45 min

Table 9

Antiparasitic activity of select compounds. Assays as described in Methods[18]. Unless otherwise stated all values are the average of three independent determinations.

Compound	EC_{50} (μM)		Selectivity[a]
	Toxo/WT	Toxo/*Cp*IMPDH	
1	1.3 ± 0.1 [b]	0.65 ± 0.03 [b]	2
26	9 ± 3	9 ± 3	1
40a	3 ± 1	0.02 ± 0.02	150
41	3.0 ± 1.0	0.9 ± 0.4	3
43	7 ± 4	4 ± 2	2
44	>25	0.5 ± 0.2	>50
45	1.1 ± 0.4	0.5 ± 0.1	2
46	8 ± 2	0.22 ± 0.04	40
48	2.4 ± 0.3	0.20 ± 0.09 [b]	34
54	2.2 ± 0.6	0.4 ± 0.3	5
55	5 ± 2	0.3 ± 0.1	16
56	1.7 ± 0.6	0.8 ± 0.4	2
57	3 ± 1	0.19 ± 0.03	14
58	21 ± 6	0.7 ± 0.1	30
62	3.3 ± 0.5	0.2 ± 0.01	15
63	3.2 ± 0.8	0.30 ± 0.3	11
64	5 ± 4	2 ± 2	3
65	2.2 ± 0.8	0.3 ± 0.1	7
66	1.7 ± 0.7	1.0 ± 0.1	1.7
70	5 ± 3	2.5 ± 0.2	1.9
72	2.1 ± 0.5	0.4 ± 0.1	5
73	4 ± 2	0.02 ± 0.02	200

[a]Selectivity is the ratio of EC_{50} Toxo/*Cp*IMPDH to EC_{50} Toxo/WT.

[b]Two determinations.